AMERICAN SOCIETY FOR MICROBIOLOGY | Molecular and Cellular Biology®

RESEARCH ARTICLE

Correction of Glycogen Synthase Kinase 3β in Myotonic Dystrophy 1 Reduces the Mutant RNA and Improves Postnatal Survival of DMSXL Mice

Mei Wang,[a] Wen-Chin Weng,[a]* Lauren Stock,[a] Diana Lindquist,[b] Ana Martinez,[c] Genevieve Gourdon,[d] Nikolai Timchenko,[e,f] Mike Snape,[g] Lubov Timchenko[a,f]

[a]Division of Neurology, Cincinnati Children's Hospital, Cincinnati, Ohio, USA
[b]Imaging Research Center, Cincinnati Children's Hospital, Cincinnati, Ohio, USA
[c]Centro de Investigaciones Biológicas (CIB, CSIC), Madrid, Spain
[d]Inserm UMR1163, Institut Imagine, Université Paris Descartes-Sorbonne Paris Cité, Paris, France
[e]Departments of Surgery, Cincinnati Children's Hospital, University of Cincinnati, College of Medicine, Cincinnati, Ohio, USA
[f]Departments of Pediatrics, University of Cincinnati, College of Medicine, Cincinnati, Ohio, USA
[g]AMO Pharma Ltd., Wonersh, Surrey, United Kingdom

ABSTRACT Myotonic dystrophy type 1 (DM1) is a multisystem neuromuscular disease without cure. One of the possible therapeutic approaches for DM1 is correction of the RNA-binding proteins CUGBP1 and MBNL1, misregulated in DM1. CUGBP1 activity is controlled by glycogen synthase kinase 3β (GSK3β), which is elevated in skeletal muscle of patients with DM1, and inhibitors of GSK3 were suggested as therapeutic molecules to correct CUGBP1 activity in DM1. Here, we describe that correction of GSK3β with a small-molecule inhibitor of GSK3, tideglusib (TG), not only normalizes the GSK3β-CUGBP1 pathway but also reduces the mutant *DMPK* mRNA in myoblasts from patients with adult DM1 and congenital DM1 (CDM1). Correction of GSK3β in a mouse model of DM1 (*HSA^{LR}* mice) with TG also reduces the levels of CUG-containing RNA, normalizing a number of CUGBP1- and MBNL1-regulated mRNA targets. We also found that the GSK3β-CUGBP1 pathway is abnormal in skeletal muscle and brain of DMSXL mice, expressing more than 1,000 CUG repeats, and that the correction of this pathway with TG increases postnatal survival and improves growth and neuromotor activity of DMSXL mice. These findings show that the inhibitors of GSK3, such as TG, may correct pathology in DM1 and CDM1 via several pathways.

KEYWORDS congenital myotonic dystrophy, GSK3β, myotonic dystrophy type 1

Myotonic dystrophy type 1 (DM1) is a complex disease affecting primarily skeletal muscle, causing myotonia, skeletal muscle weakness, and wasting (1). DM1 is caused by expanded CTG repeats in the 3′ untranslated region (UTR) of the dystrophia myotonica protein kinase gene (*DMPK*) (2). The severity of DM1 correlates with the length of CTG expansions. The longest CTG expansions are observed in patients with the congenital form of DM1 (CDM1) that affects newborn children. CDM1 is characterized by extreme muscle weakness and a weak respiratory system, which has been associated with a high mortality rate. CDM1 patients show delayed neuromotor and learning development, as well as comorbidities such as autism. Expanded CTG repeats cause the disease mainly through CUG repeats that misregulate several RNA CUG-binding proteins, including CUGBP1 (also known as a member of the family of CUGBP1 and ETR-3 like factors, CELF) and the muscleblind (MBNL) family of proteins (3). The mutant CUG-containing aggregates sequester

Citation Wang M, Weng W-C, Stock L, Lindquist D, Martinez A, Gourdon G, Timchenko N, Snape M, Timchenko L. 2019. Correction of glycogen synthase kinase 3β in myotonic dystrophy 1 reduces the mutant RNA and improves postnatal survival of DMSXL mice. Mol Cell Biol 39:e00155-19. https://doi.org/10.1128/MCB.00155-19.

Address correspondence to Lubov Timchenko, Lubov.Timchenko@cchmc.org.

* Present address: Wen-Chin Weng, Division of Pediatric Neurology, National Taiwan University College of Medicine, Taipei, Taiwan.

Received 9 April 2019
Returned for modification 2 May 2019
Accepted 1 August 2019
Accepted manuscript posted online 5 August 2019
Published 11 October 2019

MBNL1, misregulating splicing of MBNL1-regulated mRNAs (4–6). A portion of the mutant CUG repeats bind to CUGBP1 and elevate CUGBP1 protein via an increase of its stability (7). Phosphorylation of CUGBP1 by protein kinase C contributes to the increase of CUGBP1 stability (8).

CUGBP1 is a highly conserved, multifunctional protein that regulates RNA processing on several levels, including translation, RNA stability, and splicing. The increase of CUGBP1 levels observed in CDM1 leads to the delayed myogenesis *in vivo* (9, 10). Inducible overexpression of CUGBP1 in mice causes several DM1-like symptoms in skeletal and cardiac muscles (11, 12). Deletion of CUGBP1 also affects myogenesis, disrupting sarcomeric structure in the neonatal skeletal muscle, suggesting that too little or too much CUGBP1 is equally deleterious for skeletal muscle function (13). The negative effect of the loss of CUGBP1 on muscle is mediated by the disruption of multiple pathways downstream of CUGBP1, including pathways regulating cell development and extracellular matrix (13).

Multiple functions of CUGBP1 are tightly regulated by phosphorylation. Translational activity of CUGBP1 is regulated by cyclin D3–cyclin-dependent kinase 4 (CDK4)-dependent phosphorylation at S302 (14). P-S302-CUGBP1 binds to the active eukaryotic initiation translation factor 2α (eIF2α) and promotes translation of mRNAs (15). P-S302-CUGBP1 functions as an active CUGBP1 (CUGBP1^{ACT}). In DM1 myotubes, however, CUGBP1 is dephosphorylated at S302, does not bind to active eIF2α, and reduces translation of mRNAs in stress granules. Therefore, it acts as a repressor of translation (CUGBP1^{REP}) (14). The reduction of phosphorylation of CUGBP1 at S302 in skeletal muscle of patients with DM1 is caused by the reduction of cyclin D3, and delivery of cyclin D3 in DM1 myoblasts improves formation of multinucleated myotubes (16).

The reduction of cyclin D3 in DM1 skeletal muscle is caused by the increase of active glycogen synthase kinase 3β (GSK3β) kinase (17). GSK3β phosphorylates cyclin D3 at T283, marking it for degradation (18). Abnormal increase of GSK3β in DM1 muscle reduces cyclin D3, resulting in a switch of CUGBP1^{ACT} to CUGBP1^{REP}, misregulating myogenic CUGBP1 targets (13, 17). The mechanism by which GSK3β is increased in DM1 includes stabilization of GSK3β by the mutant CUG repeats (17). Correction of the GSK3β-cyclin D3-CUGBP1 pathway in the DM1 mouse model (*HSA^{LR}* mice) improves skeletal muscle strength and reduces myotonia and muscle atrophy (13, 17). A reduction of muscle pathology in *HSA^{LR}* mice treated with the inhibitors of GSK3 is associated with correction of the GSK3β-CUGBP1 axis that regulates myogenesis via several pathways, including cell development (*LEF1*, *RBM45*, and *DCX*) and extracellular matrix (*Col4A*), and due to an increase of active myogenic satellite cells (13, 17). However, a rapid reduction of the grip weakness and very effective improvement of muscle histopathology in *HSA^{LR}* mice (13, 17) suggests that the inhibitors of GSK3 have a positive effect on the reduction of the mutant CUG repeats.

In this study, we investigated whether correction of GSK3β with the inhibitor of GSK3, tideglusib (TG), reduces the mutant *DMPK* mRNA, correcting toxic events downstream of CUG repeats. Since previous studies described the abnormal GSK3β-CUGBP1 pathway in *HSA^{LR}* mice (a mouse model for an adult form of DM1, expressing ~250 CUG repeats), we also investigated if GSK3β-CUGBP1 is misregulated in DMSXL mice, which express long CUG repeats, identified in patients with severe CDM1. We also examined whether correction of GSK3β in DMSXL mice with TG has a positive effect on pathophysiology in these mice.

RESULTS

The inhibitor of GSK3, tideglusib, causes a reduction of the mutant *DMPK* mRNA. It has been shown that a primary trigger of DM1 pathogenesis is the accumulation of the mutant CUG repeats, whereas a misregulation of CUGBP1 is an early event, downstream of CUG repeats (19). To examine if the correction of GSK3β affects the primary cause of DM1, we compared the levels of the normal and mutant *DMPK* mRNA in untreated and TG-treated myoblasts from patients with adult DM1 and pediatric CDM1, informative for the Bpm1 polymorphism (20). This analysis showed that the

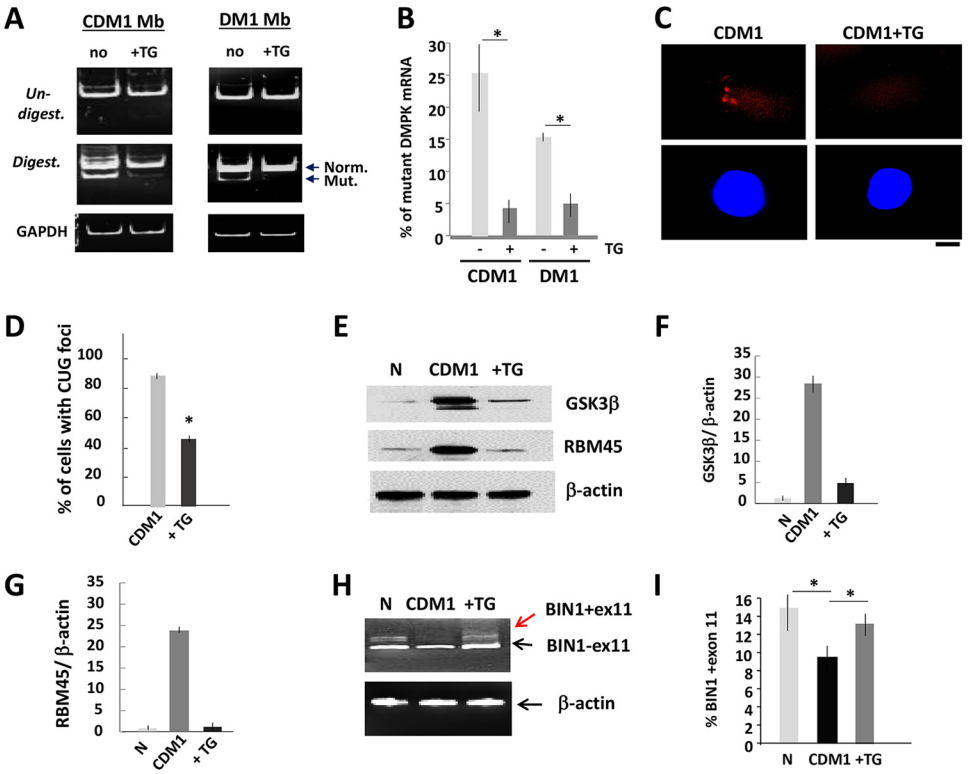

FIG 1 Reduction of the mutant *DMPK* mRNA and correction of CUGBP1 and MBNL1 activities in DM1 myoblasts treated with TG. (A) Mutant *DMPK* mRNA is reduced in CDM1 and DM1 myoblasts (Mb) treated with TG. *DMPK* levels were analyzed by qRT-PCR, and the same amounts of PCR products were digested with Bpm1. Normal and mutant *DMPK* products are shown by arrows. *GAPDH* control is shown on the bottom. (B) Quantification of the mutant *DMPK* shown in panel A. The sum of the signals for normal and mutant *DMPK* mRNA was set at 100%, and the percentages of the mutant *DMPK* were determined. (C, top) Representative FISH images of CDM1 myoblasts, treated with vehicle or TG, using CAG probe. (Bottom) Nuclei stained with DAPI. The scale bar is 5 μm. (D) Percentage of CDM1 myoblasts containing CUG foci after treatment with the vehicle or TG. Total number of analyzed cells was set at 100%. (E) GSK3β and a downstream myogenic target of CUGBP1, RBM45, are corrected in CDM1 myoblasts treated with TG. Western blot analysis shows the levels of GSK3β and RBM45 in normal (N) myoblasts and untreated and TG-treated CDM1 myoblasts. β-Actin was a loading control. (F and G) Quantification of GSK3β and RBM45 signals as ratios to β-actin levels shown in panel E. (H) Correction of *BIN1* splicing in CDM1 myotubes treated with TG. qRT-PCR of *BIN1* in normal and in untreated and TG-treated CDM1 myotubes. β-Actin was used as the control. Arrows show two isoforms with inclusion and exclusion of exon 11. (I) Quantitative analysis of *BIN1* isoform, including exon 11, shown in panel H. *, $P < 0.05$.

mutant *DMPK* mRNA is significantly reduced in the treated DM1 and CDM1 myoblasts (Fig. 1A and B). Fluorescent *in situ* hybridization (FISH) analysis confirmed the reduction of the CUG-containing foci in human CDM1 myoblasts treated with TG (Fig. 1C and D).

Examination of GSK3β showed that the GSK3β levels were increased in CDM1 myoblasts, whereas treatments with TG normalized the GSK3β levels (Fig. 1E and F). To test if correction of GSK3β with TG also corrects the CUGBP1 pathway, we examined protein levels of one of the downstream targets of CUGBP1, RNA-binding motif 45 protein (RBM45), which is associated with normal and CDM1 myogenesis (13). We found that RBM45 was also corrected in the TG-treated CDM1 cells (Fig. 1E and G).

Positive effects of TG on the reduction of the mutant *DMPK* mRNA suggest that other important feature of DM1 pathogenesis, such as abnormal splicing, should also be corrected in the treated cells. We found that the splicing pattern of *BIN1* (bridging integrator 1), regulated by MBNL1 (21), is altered in untreated CDM1 myotubes; however, the splicing of *BIN1* was normalized in CDM1 cells treated with TG (Fig. 1H and I). Based on these data, we conclude that correction of GSK3β reduces levels of the mutant *DMPK* mRNA in human CDM1 and DM1 muscle cells and has a positive effect on a number of mRNA targets regulated by CUGBP1 and MBNL1. It remains to be

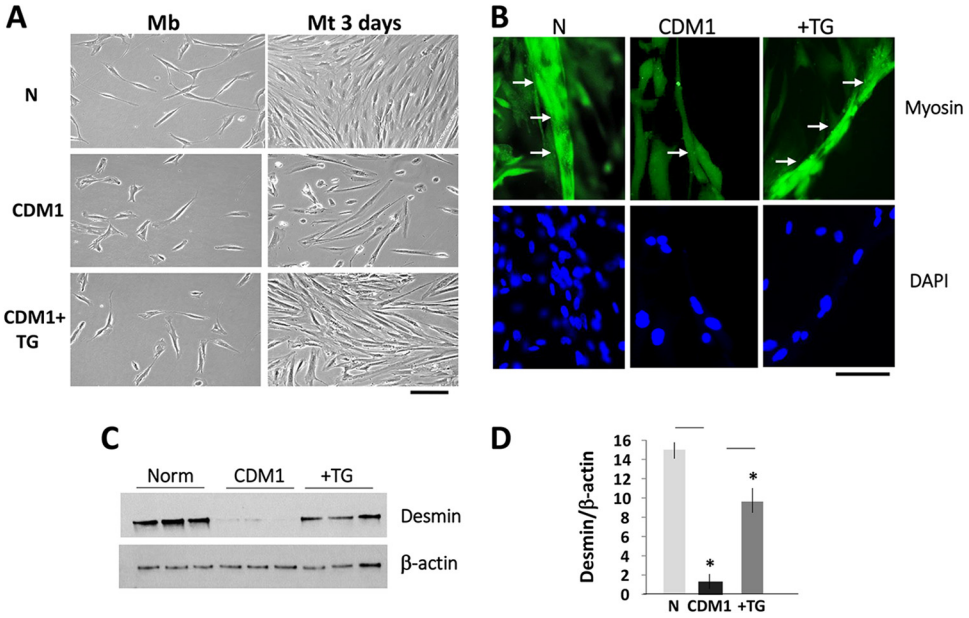

FIG 2 Correction of GSK3β improves CDM1 myogenesis. (A, left) Bright-field microscopy images of growth of normal and CDM1 myoblasts. Where indicated, CDM1 myoblasts were treated with TG prior to addition of fusion medium. (Right) Normal untreated and TG-treated CDM1 myoblasts were differentiated for 3 days. Mt, myotube. Scale bar, 100 μm. (B) Representative immunofluorescent images of normal myotubes and untreated and TG-treated CDM1 myotubes with antibodies to myosin. Arrows point to single myotubes in normal myotubes and untreated and TG-treated CDM1 myotubes. Scale bar, 25 μm. (C) Western blot analysis of a differentiation marker, desmin, in normal myotubes and untreated and TG-treated CDM1 myotubes differentiated for 2 days. β-Actin was a control for protein loading. (D) Quantification of the desmin signals as a ratio to β-actin levels shown in panel C. *, $P < 0.05$.

determined if TG corrects multiple targets of CUGBP1 and MBNL1 in human CDM1 and DM1 muscle cells.

The reduction of the mutant *DMPK* mRNA in the TG-treated CDM1 myoblasts was accompanied by improvement of CDM1 myogenesis. We found that differentiation of CDM1 myotubes treated with TG prior to addition of fusion medium is improved relative to that of untreated CDM1 cells (Fig. 2A and B). The immunofluorescence (IF) assay using antibodies (Abs) to a marker of differentiation, myosin, showed that CDM1 myotubes treated with TG are longer than those in untreated CDM1 cells (Fig. 2B). The increase of myogenesis of the treated CDM1 myotubes was also characterized by recovery of a differentiation marker, desmin (Fig. 2C and D). Thus, correction of GSK3β in CDM1 myoblasts improves myogenesis, perhaps via correction of GSK3β pathways and the reduction of the mutant *DMPK* mRNA.

Correction of GSK3β in *HSA^{LR}* mice reduces the mutant CUG repeats. We examined the effect of the correction of GSK3β on the amounts of CUG-containing RNA in *HSA^{LR}* mice treated with TG according to the protocol shown in Fig. 3A. The Northern blot analysis showed that the levels of the mutant RNA are reduced in skeletal muscle of *HSA^{LR}* mice treated for 2 weeks (2 times a week) with TG relative to those of matched mice treated with the vehicle (Fig. 3B and C). A reduction of the mutant CUG repeats in the TG-treated *HSA^{LR}* mice was accompanied by a reduction of CUG foci (Fig. 3D and E).

The GSK3β-CUGBP1 pathway was normalized in the TG-treated *HSA^{LR}* muscle, and the downstream targets of the GSK3β-CUGBP1 pathway were also corrected (Fig. 3F). CUGBP1 controls expression of mRNAs that are linked to the regulation of myogenesis, RBM45 and doublecortin (DCX) (13). Whereas RBM45 is mainly associated with cell development and differentiation (13, 22), DCX is involved in the migration of myogenic satellite cells and function of neuromuscular junctions (23, 24). As shown, expression of RBM45 and DCX was normalized in *HSA^{LR}* mice treated with TG (Fig. 3F). A reduction of

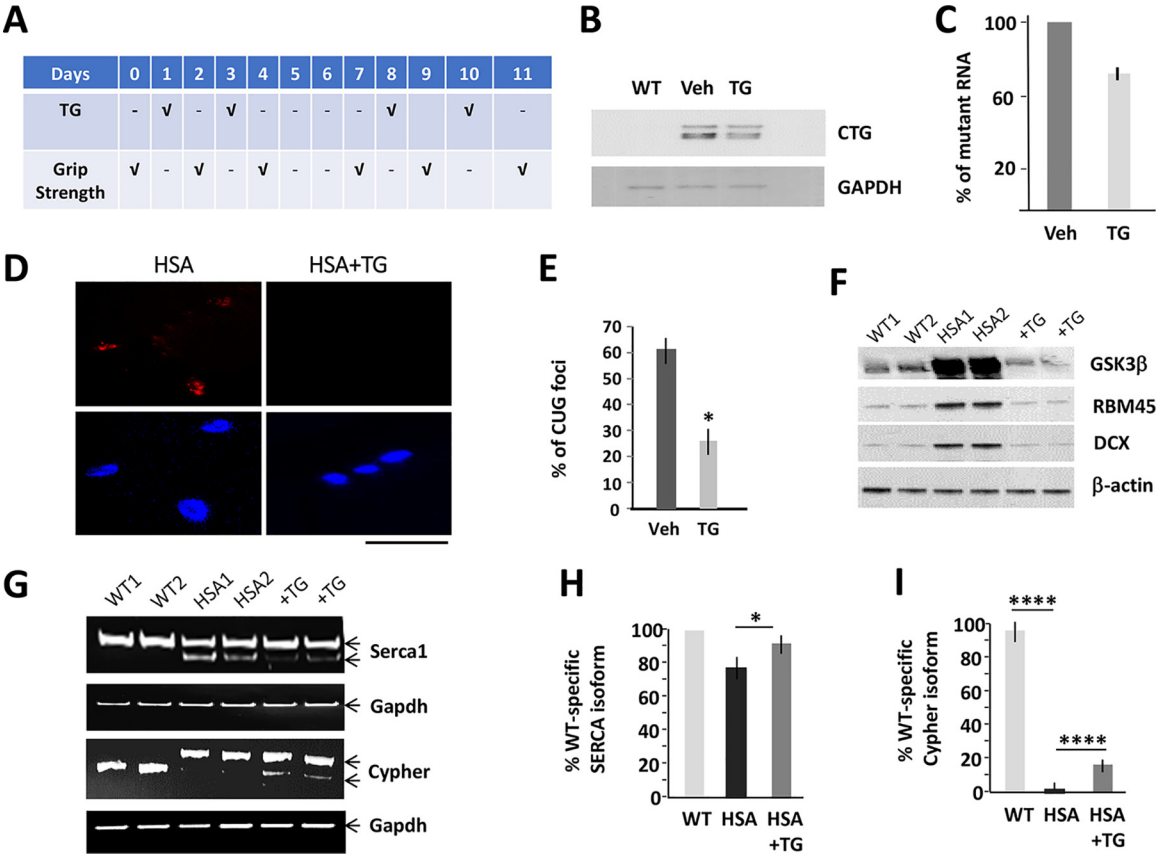

FIG 3 Correction of GSK3β reduces the levels of the mutant CUG repeats in *HSA*^{LR} mice. (A) Design of the treatment of *HSA*^{LR} mice with TG. The grip strength was measured before the course of the treatment and the day after each treatment as an outcome of the efficacy of the correction of GSK3β in *HSA*^{LR} muscle. (B) Northern blot analysis of skeletal muscle mix from matched WT and *HSA*^{LR} mice treated with the vehicle (Veh) or TG using $(CAG)_{10}$ probe. GAPDH was used as a loading control. (C) The quantification of the mutant CUG RNA in skeletal muscle of *HSA*^{LR} mice treated with TG, shown in panel B, was performed as described in Materials and Methods. (D) Representative images of FISH analysis of skeletal muscle of *HSA*^{LR} mice, treated with the vehicle or TG, using CAG probe. Nuclei were stained with DAPI. The scale bar is 100 μm. (E) The percentage of nuclear CUG foci in gastroc from 5-month-old *HSA*^{LR} mice untreated and treated with TG (2 doses, 0.1 μg/g) determined by FISH assay. (F) Western blot analysis of GSK3β and the downstream myogenic CUGBP1 targets, RBM45 and DCX, in gastroc from 5-month-old WT mice and *HSA*^{LR} mice untreated and treated with TG (2 doses, 0.1 μg/g). β-Actin was a control for protein loading. (G) Correction of misregulated splicing of *Serca1* and *Cypher* in *HSA*^{LR} mice treated with TG. *Serca1* was analyzed in TA muscle from *HSA*^{LR} mice treated i.p. with two doses of TG (0.1 μg/g). *Cypher* was analyzed in gastroc of *HSA*^{LR} mice treated four times with oral TG (0.1 μg/g). (H and I) Quantification of the signals, shown in panel G, based on three repeats, was performed as described in Materials and Methods. *, $P < 0.05$; ****, $P < 0.0001$.

CUG foci in the treated *HSA*^{LR} mice suggests that DM1-specific splicing changes are also reduced. One of the missplicing events in DM1 muscle pathology in *HSA*^{LR} mice is a misregulation of splicing of *SERCA1*. We found that the correction of GSK3β in *HSA*^{LR} mice exposed to TG leads to almost normal splicing of *SERCA1* (Fig. 3G and H). Splicing of *Cypher* was also improved in the TG-treated *HSA*^{LR} mice (Fig. 3G and I). Thus, correction of GSK3β in *HSA*^{LR} mice with TG reduces the mutant CUG RNA, decreases CUG foci, and corrects a number of CUGBP1 and MBNL1 targets. The effect of the TG treatment on global splicing events in *HSA*^{LR} muscle remains to be investigated.

We have previously shown that the correction of GSK3β in *HSA*^{LR} mice with the inhibitors of GSK3 (lithium, TDZD-8, indirubin, and BIO) has a positive effect on grip weakness (13, 17). Therefore, we examined if a reduction of the mutant CUG RNA with TG has a positive effect on grip weakness in *HSA*^{LR} mice. We found that a single dose of TG (0.1 μg/g) led to grip strength recovery in adult *HSA*^{LR} mice ~24 h after the treatment (Fig. 4A). To determine if the correction of grip weakness in *HSA*^{LR} mice depends on the TG dose, two groups ($n = 5$) of age (4 months)- and gender (males)-matched *HSA*^{LR} mice were treated with lower doses of TG (0.025 and 0.05 μg/g), as shown in Fig. 3A. There was no significant change of the grip weakness in *HSA*^{LR} mice

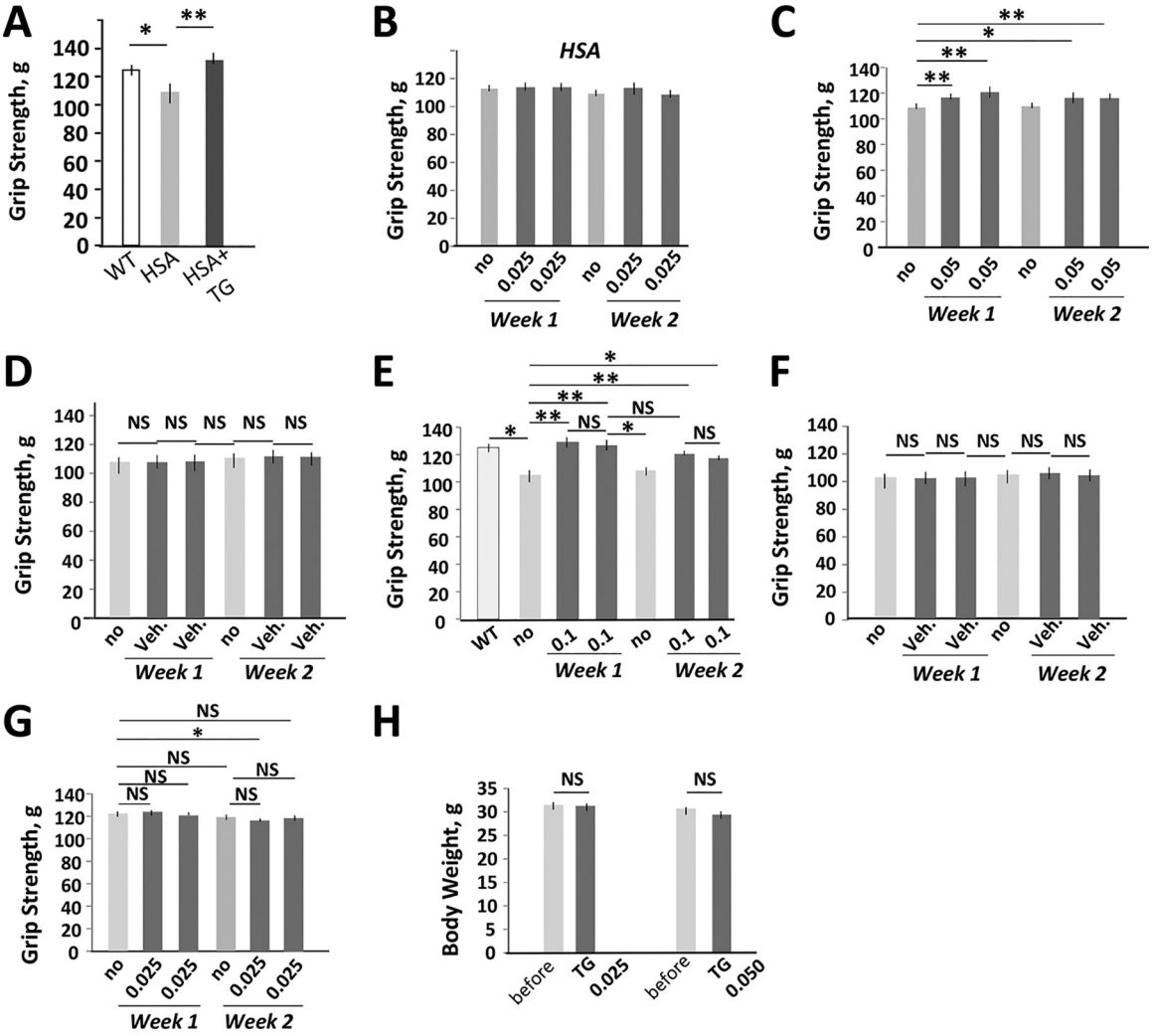

FIG 4 Reduction of the mutant CUG repeats in the TG-treated *HSA*^{LR} mice is accompanied by a quick positive effect on grip weakness. (A) A single dose of the oral TG (0.1 μg/g) corrects grip weakness in 6-month-old *HSA*^{LR} mice (females) ~24 h after treatment. The grip strength was measured before the treatment and the day after treatment. The matched WT mice were used as a control. The groups of WT and *HSA*^{LR} mice contained 5 to 6 mice. (B to D) Grip strength analysis of 4-month-old *HSA*^{LR} mice (males) ($n = 5$) treated with 0.025 μg/g of TG (B), 0.05 μg/g of TG (C), or vehicle (D). (E and F) Grip strength analysis of 6-month-old *HSA*^{LR} mice (females) ($n = 6$) treated with 0.1 μg/g of TG (E) or vehicle (F). (G) TG has no effect on the grip strength of adult WT mice. A group of WT mice (FVB, males, $n = 6$) was treated with 0.025 μg/g of TG, and the grip strength was measured according to the protocol shown in Fig. 3A. A minor (but significant) reduction of grip strength in WT mice was observed at one time point of the treatment with TG (0.025 μg/g) relative to untreated mice; however, this effect was not reproduced with a higher dose of TG (0.05 μg/g). This might occur due to a negative effect of the repetitive oral gavage procedure on mouse performance. (H) TG has no significant effect on the body weight of WT mice. WT mice ($n = 6$) were treated with TG according to the protocol described for Fig. 3A. *, $P < 0.05$; **, $P < 0.01$. NS, nonsignificant change.

treated with 0.025 μg/g TG (Fig. 4B). However, twice this dose of TG gradually increased grip strength in *HSA*^{LR} mice (Fig. 4C). Thus, the improvement of grip strength in the treated *HSA*^{LR} mice depends on the dose of the inhibitor of GSK3. We found that the grip weakness returned when the treatment was halted for 3 days, but it was recovered after reintroduction of treatment. Vehicle did not affect grip weakness in the matched *HSA*^{LR} mice (Fig. 4D).

The correction of GSK3β with TG was beneficial for the improvement of muscle strength in mice of both genders. The treatment of 6-month-old *HSA*^{LR} mice ($n = 6$, females) with a dose of 0.1 μg/g corrected grip weakness, and vehicle had no effect (Fig. 4E and F). As with a lower dose, the grip weakness returned when the treatment was stopped for 3 days, but it was improved upon reintroduction of treatment. Since grip weakness returned when the treatment stopped, we suggest that the chronic treatment with TG is required to maintain approximately normal grip strength in adult

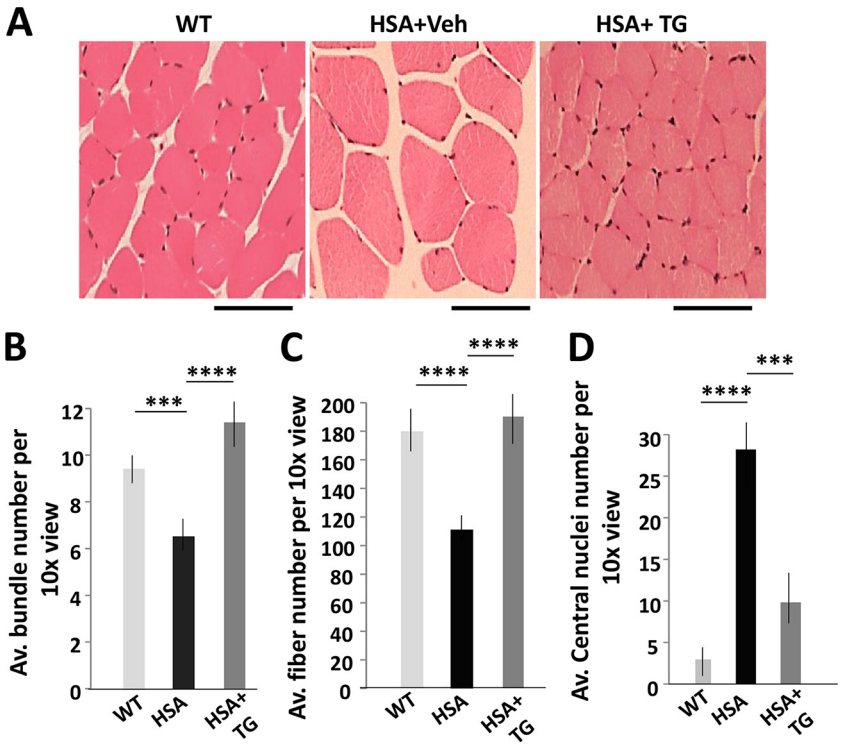

FIG 5 Correction of GSK3β in *HSA^{LR}* mice with TG reduces skeletal muscle histopathology. (A) HE staining of gastroc from WT and vehicle- and TG-treated *HSA^{LR}* mice according to the protocol described in the legend to Fig. 3A. The scale bar is 50 μm. (B to D) The average numbers of fiber bundles (B), fibers (C), and central nuclei (D) per $\times$10 view were compared in the matched WT and untreated and TG-treated *HSA^{LR}* mice (two mice per group). Calculations are based on 12 images of gastroc from WT and untreated and *HSA^{LR}*-treated mice at $\times$10. ***, $P < 0.001$; ****, $P < 0.0001$.

(4- to 6-month-old) *HSA^{LR}* mice. The same protocol of treatment of wild-type (WT) mice did not affect grip strength or body weight (Fig. 4G and H).

The longer treatments of adult 3.5-month-old *HSA^{LR}* mice (females) with TG under the same protocol (0.1 μg/g, 2 times a week) for 10 weeks and the following maintenance for 3.0 months without treatment did not have obvious negative effects on *HSA^{LR}* mice. Treated *HSA^{LR}* mice gained weight normally. The body weight of 9-month-old *HSA^{LR}* mice, treated at 3.5 months of age with TG for 10 weeks, was similar to that in untreated 9-month-old *HSA^{LR}* mice of the same gender (not shown). Although one treated mouse died, the death was not associated with the treatment, since some untreated *HSA^{LR}* mice die at different ages.

Skeletal muscle in adult *HSA^{LR}* mice is characterized by myopathy, including a variability of fiber size, with the presence of small and large hypertrophic fibers with central nuclei and by reduced bundling. We have analyzed skeletal muscle histology in *HSA^{LR}* mice treated with 0.1 μg/g TG according a protocol that reduces the mutant CUG repeats (Fig. 3A). Hematoxylin-eosin (HE) staining of gastrocnemius (gastroc) muscle showed correction of the myofiber size variability and increase of fiber bundles in *HSA^{LR}* mice treated with TG (Fig. 5A and B). The total number of fibers was reduced in untreated 6-month-old *HSA^{LR}* mice (Fig. 5C). However, the number of fibers even exceeded that in *HSA^{LR}* mice treated for 2 weeks with TG. Although centralized nuclei were still present in some myofibers in the treated *HSA^{LR}* mice, their number was significantly reduced (Fig. 5D). Positive changes in histopathology in *HSA^{LR}* gastroc were also observed after two doses of TG (0.1 μg/g). After treatment, myofiber size in these mice was normalized, the number of the centralized nuclei was reduced, and the number of fibers per bundle was increased (not shown). However, this treatment was not sufficient to correct muscle atrophy and to increase the number of bundles in *HSA^{LR}* muscle. Thus, the correction of GSK3β with TG in *HSA^{LR}* mice reduces the levels of the

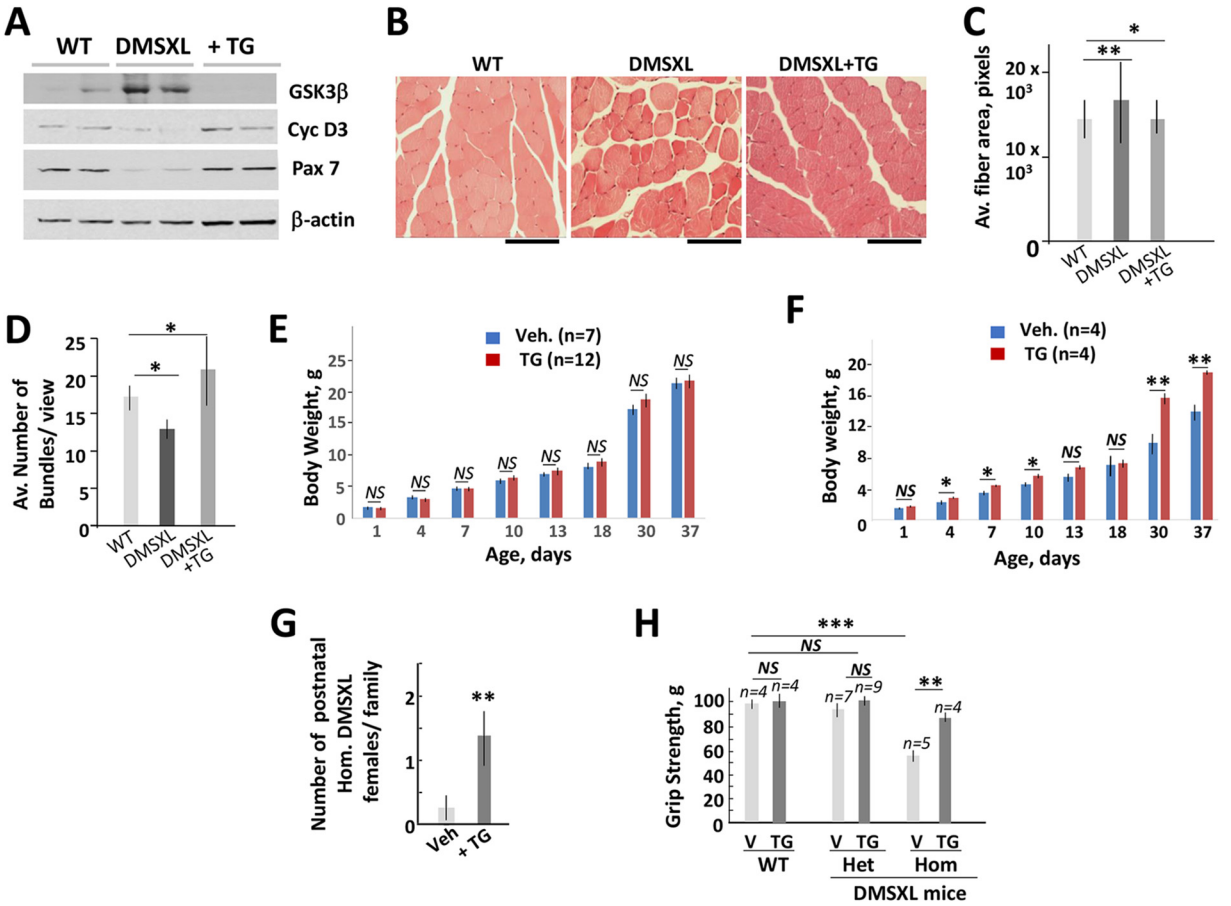

FIG 6 GSK3β-cyclin D3 pathway is abnormal in skeletal muscle of DMSXL mice. (A) Western blot analysis of protein extracts from diaphragm of the matched WT, untreated, and single-dose TG-treated (0.1 μg/g) 2.5-month-old het DMSXL mice (females) with antibodies to GSK3β and cyclin D3. The levels of a marker of muscle regeneration, Pax7, were also examined. β-Actin was a loading control. (B) HE staining of gastroc from the matched areas of the age- and gender-matched WT, untreated, and oral TG-treated (0.1 μg/g, two times a week) hom DMSXL mice is shown. Note myofiber size variability in gastroc of untreated DMSXL mice and the reduced fiber size variability in the treated DMSXL mice. The scale bar is 50 μm. (C) Normalization of fiber size in gastroc of the TG-treated 2-month-old hom DMSXL mice (0.1 μg/g, two times a week for 1 week). Two mice per group were analyzed. (D) Correction of GSK3β improves bundling in skeletal muscle of DMSXL mice. The number of bundles was counted at $\times$10 magnification for each mouse group (2 mice per group). (E and F) Comparison of the body weights of WT (E) and hom DMSXL mice (males) (F) produced by DMSXL females treated with the vehicle (2 times, 0.1 μg/g) ($n = 5$ [WT]; $n = 5$ [DMSXL]) or TG ($n = 5$ [WT]; $n = 4$ [DMSXL]) during gestation. Changes of the body weight in WT mice produced by the vehicle-treated versus TG-treated DMSXL females are not significant. (G) Average number of postnatal hom DMSXL mice (females) per family produced by the vehicle ($n = 6$)- or TG ($n = 6$)-treated DMSXL mice during gestation. (H) The grip strength is increased in hom DMSXL males produced by females treated with TG during gestation. The number of analyzed mice is shown at the top. *, $P < 0.05$; **, $P < 0.01$; ***, $P < 0.001$. NS, nonsignificant change.

mutant CUG-containing RNA, decreases the number of foci, and corrects the GSK3β-CUGBP1 pathway and at least some missplicing events. These molecular changes are accompanied by the correction of muscle atrophy, normalization of the grip strength, and reduction of myopathy.

GSK3β-CUGBP1 pathway is abnormal in DMSXL mouse model. Our previous studies showed the positive effect of the correction of the GSK3β-CUGBP1 pathway in *HSA*^{LR} mice, expressing ~250 CUG repeats that affect mice mainly in adulthood. To determine whether this pathway is misregulated by long CUG repeats, identified in severely affected patients with CDM1, we examined the levels of GSK3β in DMSXL mice. These mice express the human *DMPK* gene with more than 1,000 CUG repeats mainly in skeletal muscle, heart, and brain, affecting mice at birth (25). First, we examined GSK3β levels in diaphragms of adult DMSXL mice. Western blot analysis showed that the level of GSK3β is increased in skeletal muscle of DMSXL mice (Fig. 6A). Treatment of these mice with a single (0.1 μg/g) oral dose of TG normalized the GSK3β levels ~24 h after the treatment. One substrate of GSK3β, cyclin D3, is reduced in skeletal

TABLE 1 Survival rate of hom[a] DMSXL mice produced by DMSXL females treated with TG during lactation

DMSXL female	No. of hom DMSXL mice per family			% dead hom DMSXL
	Postnatal	Dead[a] (newborn and postnatal)	Dead in adulthood[b]	
Untreated ($n = 10$)	1.4	0.6	0.3	64.5
TG treated and lactating ($n = 3$)	1.3	0	0.3	25

[a]The number of dead hom mice includes genetically proven hom mice and underdeveloped mice that died at birth or during the postnatal period (presumably hom DMSXL mice). $P = 0.038471$.
[b]The number of hom mice that died in adulthood includes mice which died at 1.5 months and later.

muscle biopsy specimens from adult patients with DM1 and in *HSA^{LR}* mice (17). Figure 6A shows that cyclin D3 is also reduced in DMSXL diaphragm with high levels of GSK3β. As shown, cyclin D3 was recovered in skeletal muscle of DMSXL mice exposed to TG. These findings indicate that the GSK3β-cyclin D3 pathway is altered in DMSXL skeletal muscle and that TG corrects this pathway. Similar to adult *HSA^{LR}* muscle, a transcription factor, Pax-7, controlling muscle regeneration, is reduced in DMSXL skeletal muscle. However, Pax-7 was corrected in DMSXL mice treated with TG. This result suggests that the correction of GSK3β in DMSXL muscle promotes muscle regeneration.

We examined if the correction of GSK3β reduces pathophysiology in DMSXL mice. HE analysis of gastroc of adult DMSXL mice showed that skeletal muscle in these mice is characterized by a variability of myofiber size with the presence of large hypertrophic fibers (Fig. 6B). As a result, the average cross-section fiber area is increased in DMSXL muscle (Fig. 6C). Oral treatments with TG (0.1 μg/g, 2 times a week for 1 week) reduced the fiber size variability in DMSXL muscle. The number of fibers per bundle was increased in the treated mice (Fig. 6D).

Postnatal homozygous (hom) DMSXL mice have a high mortality rate. To examine if the correction of GSK3β increases the survival of postnatal DMSXL mice, lactating DMSXL females were treated with TG (0.1 μg/g, 3 times between 1 and 7 days after delivery of newborn pups). We found that all hom DMSXL mice survived during the postnatal period when the lactating DMSXL females ($n = 3$) were treated with TG (Table 1). In contrast, almost half (42.9%) of postnatal hom DMSXL mice produced in untreated families ($n = 10$) died ($P < 0.05$). One hom DMSXL mouse in the treated families died at an age of 2.5 months. Thus, postnatal treatment of DMSXL mice with TG increases the survival rate of underdeveloped DMSXL mice.

Since some hom DMSXL mice die at birth, we tested the effect of the prenatal correction of GSK3β on the survival and growth of the underdeveloped DMSXL mice. A group of gestating DMSXL females ($n = 6$) was treated with oral TG (0.1 μg/g, two times during 11 to 16 days of gestation), whereas a second group ($n = 6$) was treated with vehicle. The total body weight of DMSXL offspring was monitored from 1 to 37 days of age. We found a significant improvement of postnatal growth of hom DMSXL mice (males) produced by TG-treated females (Fig. 6F) but not the matched WT or heterozygous (het) DMSXL offspring (Fig. 6E and data not shown). We also attempted to examine the postnatal growth of hom DMSXL females generated by DMSXL mice treated with TG during gestation. However, only a single postnatal hom DMSXL female (out of 60 mice in 6 crosses) was identified in vehicle-treated families. In contrast, 8 postnatal hom DMSXL females were identified in the TG-treated families (Fig. 6G). Thus, correction of GSK3β in DMSXL mice during gestation increases the number of hom DMSXL females. We are planning to investigate the larger number of DMSXL families to determine if there is a gender-dependent effect of the correction of GSK3β on the survival of postnatal DMSXL mice.

Careful monitoring of postnatal mice suggested that the increase of hom DMSXL females in the TG-treated families is due to increased survival during the postnatal period because homozygosity is not embryonic lethal and because almost half of untreated hom mice die during the postnatal period (Table 1). However, we cannot

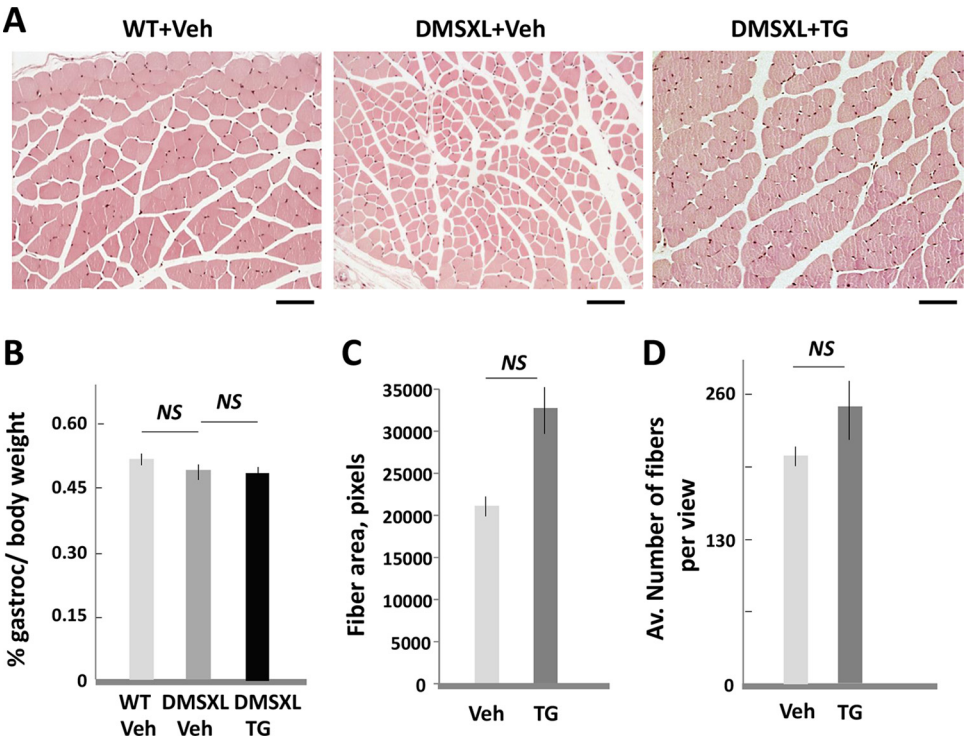

FIG 7 (A) HE staining of gastroc from the matched hom DMSXL mice (6-week-old males), produced by the vehicle- or TG-treated DMSXL females. The matched WT littermates, produced in the vehicle-treated families, were analyzed as a control. The scale bar is 50 μm. Note the presence of small fibers in the gastroc from hom DMSXL mice, produced by the vehicle-treated females. (B to D) The gastroc weights, determined as a percentage of whole body weight (B), the average cross-sectional fiber areas (C), and the average numbers of fibers per $\times$10 view (D) were compared in gastroc from 6-week-old hom DMSXL mice (males) produced by DMSXL females treated with the vehicle or TG during gestation. Two mice per group were analyzed. The fiber area and the number of fibers in the vehicle-treated mice were corrected to the gastroc weight. NS, nonsignificant change.

exclude that the prenatal treatments with TG have a positive effect on the embryonic development of hom DMSXL mice.

We found that grip strength was significantly increased in 6-week-old hom DMSXL mice generated by DMSXL females treated with TG during gestation relative to that of matched hom DMSXL mice ($n = 4$, males) produced by vehicle-treated females (Fig. 6H). However, WT and het DMSXL littermates of the same age and gender (males) had comparable grip strength in the vehicle- and TG-treated families.

HE analysis of skeletal muscle of 6-week-old hom DMSXL mice produced by TG-treated females showed that their fiber size is larger than that in matched mice from the vehicle-treated families (Fig. 7A). We also found that gastroc weight is much higher in hom DMSXL mice produced by TG-treated females than that in mice produced by vehicle-treated females. However, comparison of the percentages of muscle weight to body weight showed no significant differences in the two groups (Fig. 7B). Thus, the increase of muscle in hom DMSXL mice generated by the TG-treated females is due to increase of total body weight. Therefore, even if the fiber size in hom DMSXL mice from the TG-treated families is increased, there is no significant difference from the average fiber size in the offspring from the vehicle- and TG-treated mice after the correction of the fiber size to the gastroc weight in both groups (Fig. 7C). The number of fibers per view was not significantly changed in the gastroc from hom DMSXL mice produced by the vehicle- or TG treated females (Fig. 7D). Taken together, correction of GSK3β in gestating DMSXL mice increases the survival of postnatal hom DMSXL females and has a strong positive effect on the postnatal growth and strength of hom DMSXL mice.

TG-mediated correction of GSK3β-CUGBP1 pathway in brain of DMSXL mice improves the neuromotor activities. A delay of speech and neuromotor development

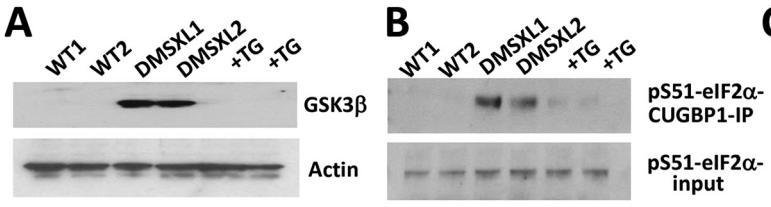

C

Short name	Long name	Fold change	P value
RBM45	RNA-binding motif 45 (BC3H1 cDNA encoding RNA-binding region RNP-1)[a]	19.751	2.01E-05
HNRPDL	heterogeneous nuclear ribonucleoprotein D-	1.535	4.17E-02
SRSF2	serine/arginine-rich splicing factor 2	1.554	1.51E-02
SMN1	survival motor neuron 1[a]	1.524	3.46E-02
MBNL3	muscleblind-like 3[a]	1.557	4.42E--02
RBM12	RNA-binding motif 12	1.545	2.92E-02

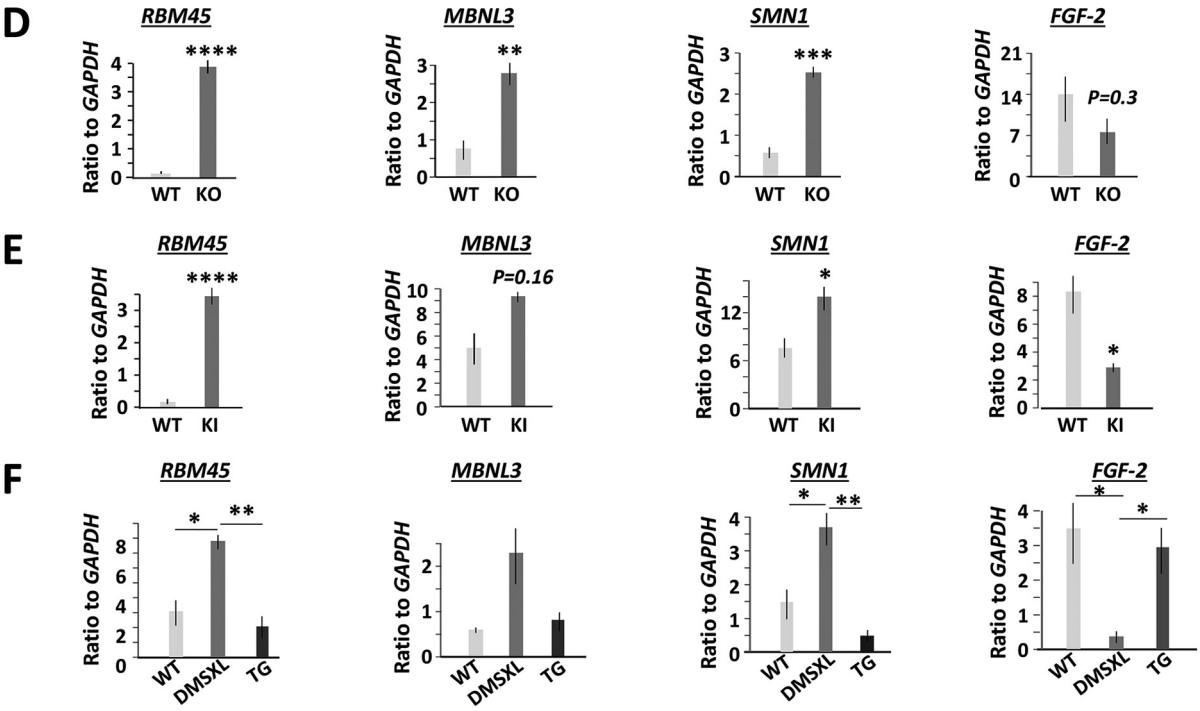

FIG 8 The GSK3β-CUGBP1 pathway is abnormal in DMSXL brain. (A) TG corrects the levels of GSK3β in the brains of DMSXL mice. Western blotting of protein extracts from the whole brains of 2-month-old WT and untreated and treated with TG hom DMSXL mice with antibodies to GSK3β and actin as a control. (B) Correction of GSK3β restores CUGBP1 activity in the brains of DMSXL mice. (Top) Interactions of CUGBP1 with inactive p-S51-eIF2α in the cytoplasmic extracts from the whole brains of 2-month-old (male) WT, untreated, and TG-treated (0.1 μg/g, 2 times) hom DMSXL mice were examined by the IP-Western blot analysis. (Bottom) Input of p-S51-eIF2α prior to precipitation. (C) The list of mRNAs encoding RNA-binding proteins altered in the whole brain of neonatal hom *Celf1* KO mice, determined by the global microarray analysis of gene expression (13). Superscript letter "a" indicates genes examined in this study. (D) Confirmation of the altered expression of mRNAs, downstream of CUGBP1, in 0- to 5-day-old *Celf1* KO brains by qRT-PCR. *Rbm45* and *Smn1* were examined in hom *Celf1* KO brains, whereas *Mbnl3* and *Fgf-2* were analyzed in het *Celf1* KO mice. (E) *Rbm45*, *Mbnl3*, *Smn1*, and *Fgf-2* show similar patterns of expression in the brains of 1-month-old CUGBP1 S302A-KI mice (males) that contain inactive $CUGBP1^{REP}$ due to a mutation of the GSK3β-cyclin D3-CDK4 site. *Rbm45* was measured by qRT-PCR in het CUGBP1-S302A-KI brains, whereas *Mbnl3*, *Smn1*, and *Fgf-2* were tested in the brains of hom CUGBP1-S302A-KI mice. (F) Correction of GSK3β normalizes the downstream targets of CUGBP1 in DMSXL brains. Shown is the qRT-PCR analysis of *Mbnl3*, *Fgf-2*, and *Smn1* in the whole-brain extracts from neonatal WT mice, untreated hom DMSXL mice, and hom DMSXL mice produced by females treated 1 to 2 times with TG during gestation. *Rbm45* was measured in the whole brains of 6-week-old WT mice, untreated hom DMSXL mice, and hom DMSXL mice produced by TG-treated females during gestation. *, $P < 0.05$; **, $P < 0.01$; ***, $P < 0.001$; ****, $P < 0.0001$.

is one of the features of CDM1 (1). Therefore, we examined if the neurological defects in DMSXL mice are associated with an abnormal GSK3β-CUGBP1 pathway. Figure 8A shows that GSK3β is increased in the whole-brain protein extracts from DMSXL mice relative to that of matched WT mice. The increase of GSK3β in DMSXL brain suggests misregulation of CUGBP1 activity. The main alteration of CUGBP1 activity is dephosphorylation of CUGBP1 at S302, which converts active protein to a repressor (called $CUGBP1^{REP}$). Since the amount of $CUGBP1^{REP}$ can be determined by its interaction with inactive (p-S51) eIF2α (13, 17), we compared the amounts of p-S51-eIF2α bound to CUGBP1 in the protein extracts from the matched WT and DMSXL brains. CUGBP1 was immunoprecipitated (CUGBP1-IP), and the levels of p-S51-eIF2α were determined in the CUGBP1-IPs by Western blot assay. This analysis showed that repression activity of $CUGBP1^{REP}$ is increased in DMSXL brains and that treatments with TG reduce this repression activity (Fig. 8B). Since

CUGBP1^{REP} is mainly observed in stress granules (14), the presence of stress-related CUGBP1^{REP} in brains of DMSXL mice suggests that this isoform of CUGBP1 disrupts brain development and function due to cellular stress.

Our recent analysis of molecular pathways in brains from hom *Cugbp1* (*Celf1*) knockout (KO) mice showed that CUGBP1 regulates brain cell development and differentiation, nucleotide metabolism, cell import and export, protein folding, and protein degradation (13). Loss of CUGBP1 in brain alters expression of 88 ion channel transporters, including those involved in calcium and potassium transport, and G-protein-coupled receptors regulating postsynaptic membrane potential. Thus, misregulation of the GSK3β-CUGBP1 pathway in brain might affect multiple brain-specific mRNAs that directly or indirectly control RNA homeostasis, ion transport, neurogenesis, and protein degradation and folding.

The list of mRNAs altered in *Celf1* KO brain includes several mRNAs encoding RNA-binding proteins: Rbm45, spinal motor neuron 1 (Smn1), and muscleblind 3 (Mbnl3) (Fig. 8C). Previously, we found that the correction of GSK3β with TG normalizes RBM45 expression in CDM1 myoblasts and in *HSA^{LR}* muscle (Fig. 1E and G and 3F). However, RBM45 has been identified as a protein that is involved in early brain development (22). Analysis of gene expression in *Celf1* KO brains showed that whereas multiple brain mRNAs show subtle changes after CUGBP1 loss, *Rbm45* mRNA was upregulated almost 20-fold (Fig. 8C). SMN deficiency affects the formation and function of axons and dendrites, causing the loss of motor neurons and resulting in spinal muscular atrophy (SMA) (26). Interestingly, peripheral neuropathy occasionally occurs in DM1 patients, and DMSXL mice develop peripheral neuronopathy with a reduced number of lumbar motor neurons (27). MBNL3 belongs to the MBNL family of proteins associated with DM1 pathology. MBNL3 is involved in myogenesis in adult mice and is expressed during early embryonic development in the neural tube (28–30).

We have confirmed abnormal expression of *Rbm45*, *Mbnl3*, and *Smn1* in *Celf1* KO brains by quantitative reverse transcription-PCR (qRT-PCR) (Fig. 8D). One of the mRNAs, misregulated in *Celf1* KO brains, encodes fibroblast growth factor 2 (FGF-2), which is linked to neurogenesis (31). qRT-PCR analysis confirmed that *Fgf-2* is reduced in the brains of *Celf1* KO mice (Fig. 8D).

We also obtained additional evidence that *Rbm45*, *Smn1*, *Mbnl3*, and *Fgf-2* expression in brain depends on CUGBP1. We found that these mRNAs are similarly misregulated in the brains of the mutant mice in which the CUGBP1 site, phosphorylated by the GSK3β-cyclin D3-CDK4 pathway (S302), was mutated to alanine (S302A knock-in [CUGBP1-S302A-KI] mice) (Fig. 8E). In CUGBP1-S302A-KI mice, a replacement of S302 with alanine produces a CUGBP1^{REP} isoform that cannot be converted into CUGBP1^{ACT}, mimicking the accumulation of CUGBP1^{REP} in the brains of DMSXL mice. The lack of CUGBP1 activity in CUGBP1-S302A-KI mice was confirmed by the examination of CUGBP1 interactions with inactive p-S51-eIF2α (32). qRT-PCR analysis of the downstream targets of CUGBP1 in brain (*Rbm45*, *Mbnl3*, *Smn1*, and *Fgf-2*) assessed by the analysis of gene expression in *Celf1* KO brains showed that these mRNAs are also altered in CUGBP1-S302A-KI brains.

To test if the putative targets of CUGBP1 are misregulated in DMSXL brains, we have examined expression of *Rbm45*, *Mbnl3*, *Smn1*, and *Fgf-2* in neonatal brains of untreated and prenatally TG-treated hom DMSXL mice. As shown in Fig. 8F, these mRNAs have abnormal expression in the untreated DMSXL brains. However, the expression of *Rbm45*, *Mbnl3*, *Smn1*, and *Fgf-2* was corrected in the brains of hom DMSXL mice produced by TG-treated females. These findings show that the correction of GSK3β in gestating DMSXL females normalizes the GSK3β-CUGBP1 pathway in brains of DMSXL offspring and improves expression of the genes downstream of CUGBP1.

Since anxiety and memory deficits have been reported in DMSXL mice (33), we examined if prenatal treatments with TG correct these deficits in DMSXL mice. Using the open-field test, we found that adult hom DMSXL mice travel a shorter distance with reduced horizontal and vertical activities relative to those of WT mice (Fig. 9A to C).

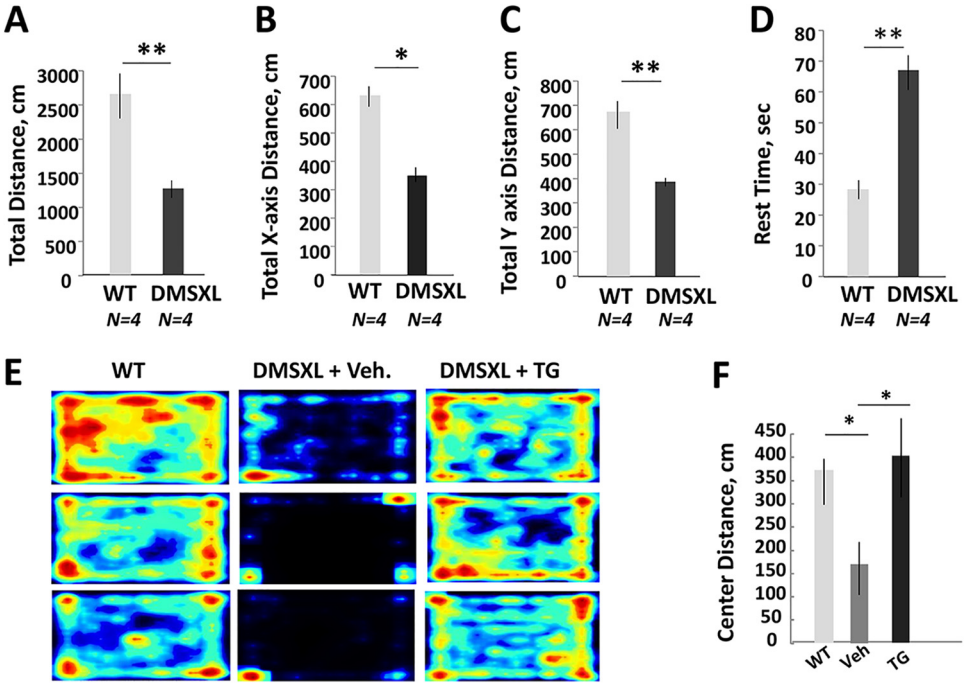

FIG 9 Reduction of neuromotor activity in adult hom DMSXL mice. (A to D) Total distances (A), total horizontal distances (B), total vertical distances (C), and rest times (D) were compared in the matched 4.5-month-old WT and hom DMSXL mice ($n = 4$ per group, females) using the open-field test. (E and F) Open-field test (heat maps) and center distance travelled by 6-week-old WT and hom DMSXL males produced by DMSXL mice treated with the vehicle or TG (0.1 μg/g) during gestation. Four to five mice in each group were examined for 5 min. *, $P < 0.05$; **, $P < 0.01$.

Hom DMSXL mice also moved less and needed more rest time than matched WT littermates during exposure for 5 min in the open-field test (Fig. 9D). Examination of 2-month-old hom DMSXL mice, produced by TG-treated females ($n = 4$, males), by the open-field test showed that these mice were more active and travelled a longer total distance; however, due to variability of phenotype and a relatively low number of hom mice in the DMSXL line, these differences were not significant. The duration of vertical movement and vertical episode counts were significantly increased in DMSXL mice produced by TG-treated females relative to those from vehicle-treated mice (not shown). Hom DMSXL mice in the TG-treated families also had markedly reduced anxiety, as judged by increased travelled distance in the center of the cage during the 5-min test (Fig. 9E and F). As shown, untreated WT mice freely travelled in the cage, including the central area of the cage. However, 6-week-old hom DMSXL mice produced by vehicle-treated DMSXL females mainly travelled near the walls and preferred to stay in the corners of the cage. In contrast, hom DMSXL mice (males) generated by TG-treated females showed a remarkable increase in the travelled distance in the center of the cage.

We compared general activity of 6-week-old het DMSXL mice in vehicle- and TG-treated families using the open-field test. Het DMSXL mice produced by TG-treated females were more active and travelled a longer total distance during the 5-min test than those from vehicle-treated mice (Fig. 10A). They also showed increased horizontal and vertical activity, increased margin distance legacy, and increased total activity counts (Fig. 10B to E). Interestingly, neuromotor measures in het DMSXL mice produced by TG-treated females exceeded those in matched untreated WT mice. The reason for these differences remains to be determined.

Thus, the GSK3β-CUGBP1 pathway is misregulated in brains of DMSXL mice. Correction of this pathway with TG in gestating DMSXL females reduced anxiety of DMSXL mice.

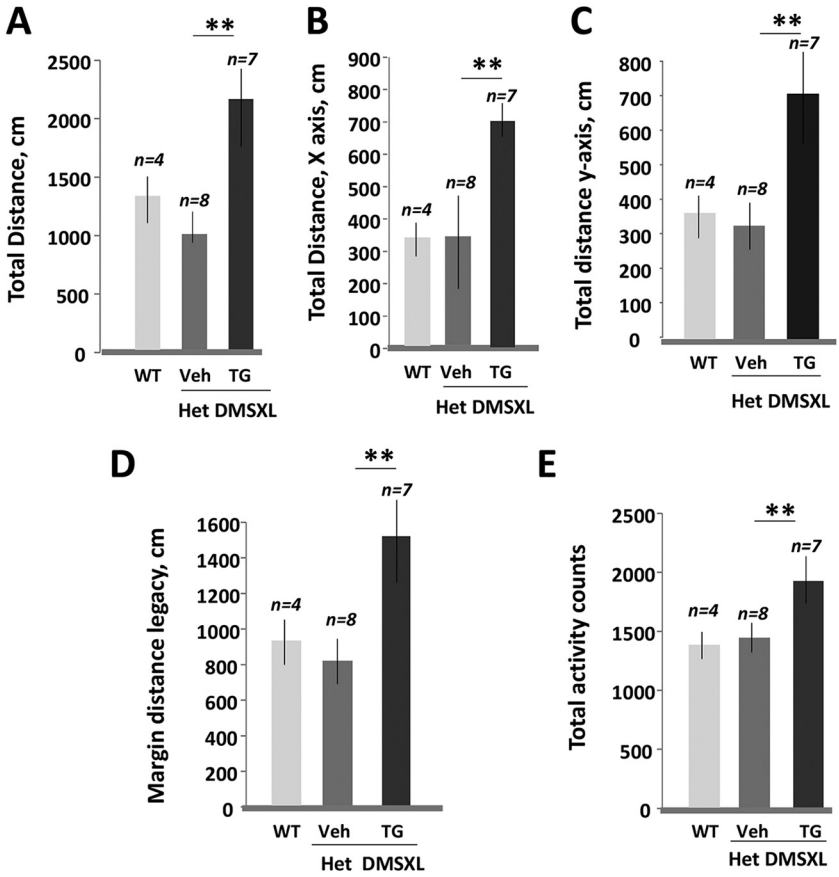

FIG 10 Open-field test of het DMSXL mice produced by females treated with the vehicle or TG during gestation. The total distances (A), total horizontal distances (B), total vertical distances (C), margin distance legacies (D), and total activity counts (E) were compared between untreated 6- to 8 week-old WT mice and het DMSXL mice produced by the vehicle- and TG-treated females. **, $P < 0.01$.

DISCUSSION

The most significant result of this study is that a correction of GSK3β with small-molecule inhibitor TG reduces the mutant *DMPK* mRNA in human myoblasts from patients with the adult form of DM1 and from pediatric patients with CDM1 (Fig. 1A and B). This finding suggests that TG reduces CDM1 and DM1 pathology via (i) correction of GSK3β activity and GSK3β substrates, including cyclin D3-CUGBP1 pathways, and (ii) via reduction of the mutant mRNA, which in turn should also correct GSK3β (Fig. 11). Therefore, the inhibitors of GSK3, such as TG, might have a broad positive effect on DM1 and CDM1 pathology, targeting both the primary toxic event (accumulation of CUG repeats) and early toxic events downstream of CUG repeats (misregulation of GSK3β and CUGBP1). The correction of GSK3β also has a positive effect on missplicing. While missplicing of *Serca1* in untreated HSA^{LR} mice was not as strong as previously described, the altered splicing pattern was in agreement with previous reports (34). Variability of the missplicing efficiency in untreated HSA^{LR} muscle is likely due to instability of CTG repeats and variability of the phenotype of HSA^{LR} mice. Although we found an improvement of a number of CUGBP1 and MBNL1 targets by the TG treatment, the detailed pathway analysis, including global splicing events in human CDM1 and DM1 muscle cells and in HSA^{LR} muscle treated with TG, is required to determine if correction of GSK3β in DM1 improves all targets regulated by CUGBP1 and MBNL1.

The detailed mechanism by which TG reduces the toxic CUG-containing RNA remains to be identified. Our previous study showed the normalization of the levels of RNA helicase p68 in HSA^{LR} mice treated with an analog of TG, TDZD-8 (35). Thus, it is

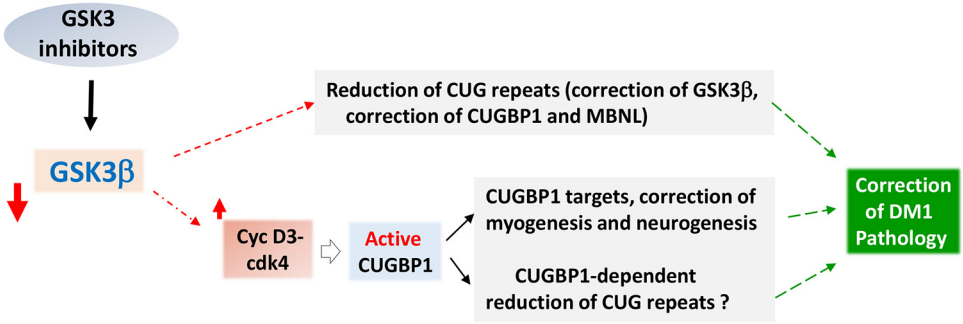

FIG 11 Diagram showing possible mechanistic effect of the inhibitors of GSK3 on DM1 pathogenesis. According to the findings in the current study and previous work, the inhibitors of GSK3 normalize the levels of GSK3β and cyclin D3 and convert inactive CUGBP1^{REP} into active CUGBP1^{ACT} in DM1. The correction of this pathway occurs in skeletal muscle and in brain, and possibly in other tissues, affected in DM1, and the downstream targets of CUGBP1 in skeletal muscle and in brain might be corrected. In addition, TG reduces the mutant *DMPK* mRNA. The mechanisms of this effect remain to be determined. However, it is likely that correction of CUGBP1 is a part of these mechanisms. It is expected that the reduction of the mutant *DMPK* mRNA will reduce main toxic events downstream of the mutant CUG repeats and might include the feedback normalization of GSK3β.

possible that treatment with TG corrects pathways improving degradation of the mutant *DMPK* mRNA. Other pathways that might be involved in the reduction of the mutant *DMPK* mRNA in human DM1 cells and in *HSA^{LR}* muscle might be determined by the analysis of the global gene expression in DM1/CDM1 cells and in *HSA^{LR}* mice treated with TG.

Broad positive effects of the inhibitors of GSK3 might explain a rapid effect of TG and TDZD-8 (17) on the correction of muscle atrophy and efficient recovery of grip strength in *HSA^{LR}* mice. Such a positive effect could be associated with normalization of many genes downstream of the GSK3β-CUGBP1 pathway (13). It has been shown that CUGBP1 might contribute to the control of muscle function via control of synaptogenesis in neuromuscular junctions and Ca^{2+} homeostasis needed for muscle activity. This suggestion is supported by (i) correction of the components of the GSK3β-CUGBP1 pathway (GSK3β, cyclin D3, and CUGBP1^{REP}) in 2 to 4 days after the treatment of *HSA^{LR}* mice with the inhibitors of GSK3, TDZD-8, or TG and (ii) by the identification of several muscle mRNAs (*RBM45*, *DCX*, and *Col13*) downstream of CUGBP1 which are involved in the neurogenesis and the function of neuromuscular junctions (13, 24, 36). In agreement, myogenic downstream targets of CUGBP1, such as RBM45 and DCX, were corrected in skeletal muscle of *HSA^{LR}* mice treated with TG (Fig. 3F). In addition to the correction of the GSK3β-CUGBP1 pathway, other pathways downstream of the toxic CUG repeats are likely corrected in the TG-treated *HSA^{LR}* mice due to reduction of the mutant CUG repeats. Studies of global gene expression in TG-treated DM1 models might show other GSK3β-dependent pathways affected by TG and possible off-target activity.

The second critical finding of our study is the identification of the defective GSK3β-CUGBP1 pathway in DMSXL mice expressing long CUG repeats in the CDM1 range. In contrast to *HSA^{LR}* mice, which express ~250 CUG repeats, long CUG repeats in the DMSXL model affect mice at birth, causing a delay of development and postnatal death.

Since significant numbers of postnatal hom DMSXL mice die and survivors are characterized by reduced growth and weakness, it is important that correction of GSK3β in gestating DMSXL mice increases the survival of postnatal hom DMSXL offspring (females). Postnatal treatments also had a positive effect on the survival rate of hom DMSXL mice. Whether the prenatal treatments with TG have any effect on the improvement of the embryonic development of hom DMSXL mice remains to be studied.

The postnatal underdeveloped DMSXL mice of both genders, produced by DMSXL females with corrected GSK3β, showed improved growth and increased strength.

TABLE 2 Frequency of WT, het, and hom DMSXL littermates, based on 33 crosses of het DMSXL mice[a]

Genotype[b]	No.	%
WT	42	25
Het	99	58.9
Hom	22	13.1

[a]WT and het DMSXL mice were counted after genotyping. A total of 168 mice were examined.
[b]The number of hom DMSXL mice includes mice confirmed by genotyping and presumably hom mice based on their small size and mortality at 0 to 8 days after birth. The genotyping of some dead (likely hom) DMSXL mice after birth was impossible due to tissue deterioration. Some neonatal hom DMSXL mice that died at birth might not be counted.

Whereas body weight and the grip strength of underdeveloped DMSXL mice in the TG-treated families were improved, these parameters remained below those in matched untreated WT mice (Fig. 6E, F, and H and data not shown). This suggests that the prenatal doses of TG have to be increased or the treatment has to continue during the postnatal period to improve the growth and strength of DMSXL mice to the levels observed in WT mice.

Although the effect of the correction of GSK3β with TG overall was positive for hom DMSXL mice, there was variability of phenotype recovery in DMSXL mice produced by the TG-treated mice. For instance, some hom DMSXL females in the drug-treated group showed strong improvement of body weight; however, some matched hom mice still had low body weight (data not shown). The reasons for such variability of recovery in DMSXL mice produced by the TG-treated females remain to be determined. This variability might be associated with the instability of CTG repeats (37) and contribution of additional factors to the disease, such as methylation in the *DMPK* locus (38).

Since mutant CUG repeats are expressed in DMSXL mice in all tissues in which DMPK is expressed, we examined the GSK3β-CUGBP1 pathway in skeletal muscle and in brain. We found that this pathway is disrupted in both skeletal muscle and in brain in DMSXL mice. Several mRNAs downstream of CUGBP1 that are important for brain function (*Rbm45*, *Mbnl3*, *Smn1*, and *Fgf-2*) were misregulated in DMSXL mice (Fig. 8F). The correction of GSK3β with TG normalized these mRNAs in DMSXL brains, suggesting that TG or other inhibitors of GSK3 correct central nervous system defects in DM1. In agreement, anxiety was corrected in hom DMSXL mice produced by the TG-treated DMSXL females.

In summary, this study shows that the correction of GSK3β has positive effects on the primary cause of DM1 and CDM1 pathogeneses (the mutant CUG repeats) and on the early downstream target of CUG repeats, CUGBP1. The correction of GSK3β with TG is beneficial for skeletal muscle and brain phenotypes in DM1 mouse models. The developing clinical trials will decipher if GSK3 inhibitors, such as TG, have therapeutic benefits in patients with DM1 and CDM1.

MATERIALS AND METHODS

Mice. Hom *HSA^{LR}* mice (FVB background), line 20LRb (5), were obtained from C. A. Thornton (University of Rochester). Age- and gender-matched WT mice (FVB background; Jackson Laboratory) were used as controls. DMSXL mice were obtained from G. Gourdon (France). Het DMSXL mice (on mixed C57B plus FVB background) were bred to maintain the line. Genotyping of DMSXL mice was performed using the following primers: FBF, 5′-TCCTCAGAAGCACTCATCCG-3′; FBWDR, 5′-ACCTCCATCCTTTCAGCACC-3′; and FBFBR, 5′-AACCCTGTATTTGACCCCAG-3′. WT and het DMSXL littermates were used as controls for hom DMSXL mice. The number of hom DMSXL mice in this strain was low (13.1% versus the expected 25%) due to postnatal and possible prenatal mortality (Tables 1 and 2). Since large numbers of hom DMSXL mice were born, the homozygosity seems not to be embryonic lethal. Careful monitoring of these mice suggests that the reduction of hom DMSXL mice is mainly due to postnatal mortality, because almost half of postnatal hom mice died (Table 1). Some underdeveloped (presumably hom) DMSXL mice die immediately after birth. It is also possible that some underdeveloped hom DMSXL mice die *in utero*. To increase the number of hom DMSXL mice, het DMSXL mice were crossed with hom mice; however, the majority of newborn pups in these crosses died after birth.

Maintenance and genotyping of *Celf1* KO mice were described previously (13). CUGBP1 S302A-KI mice were generated as described previously (32). Mice were genotyped with the following primers. The sequence of the forward primer is 5′-TTCCTGTTGGCAAGAGAAGGCAAG-3′. The sequence of the reverse

primer is 5′-ATGACAACCAGGGCTTGCCCATTA-3′. The whole brains were collected from WT and hom littermates and used for histological and molecular analyses.

Compounds and treatments. TG from AMO Pharma was used at different doses as indicated. Initial experiments were performed using TG provided by A. Martinez. For the treatments of *HSA^{LR}* mice, TG was administered at doses of 0.025, 0.05, and 0.1 μg/g dissolved in Labrasol using oral gavage.

To treat DMSXL mice, TG, dissolved in Labrasol, was administered at a dose of 0.1 μg/g using oral gavage. Mouse tissues were collected after the last treatment at approximately 24 to 48 h. Where indicated, TG dissolved in dimethyl sulfoxide (DMSO) was administered intraperitoneally (i.p.) in DMSXL or *HSA^{LR}* mice. When two doses of TG were used, the doses were administered a day apart and the mouse tissues for the analysis were collected 24 h after the second dose. In the experiments examining the effect of TG on the survival rate of DMSXL mice during the postnatal period, the lactating females initially were treated with TG using oral gavage. However, some treated females stopped feeding pups, presumably due to distress associated with the oral treatment procedure. The same problem was observed in the treatment of young (1- to 2-month-old) hom DMSXL mice. Therefore, the lactating DMSXL females were treated with TG (0.1 μg/g) i.p. 3 times between 1 and 7 days after delivery of newborn pups. There was no problem treating adult het DMSXL mice using oral gavage.

Gestating DMSXL mice were treated with oral TG (0.1 μg/g dissolved in Labrasol) two times between 11 and 17 days of gestation. In some experiments, one treatment of the gestating DMSXL mice with the oral TG (0.1 μg/g dissolved in Labrasol) was performed between 13 and 16 days of gestation. Control DMSXL or *HSA^{LR}* mice were treated with Labrasol.

Cultured myoblasts were treated with two doses of TG (1.6 μg/ml, dissolved in DMSO) a day apart, and the cell protein or RNA extracts were collected 24 h after addition of the second dose of the drug. In the experiments using myotubes, TG was added to the growing myoblasts at a dose of 1.6 μg/ml, the growth medium was changed the next day, and the fusion medium was added the following day. If two doses of the drug were used, they were added to the growing myoblasts a day apart, the growth medium was changed the day after the second treatment, and the fusion medium was added the following day.

Histological analyses. Transverse muscle sections from the matched gastroc were stained with HE at the Pathology Laboratory at CCHMC. To assess the average fiber size, the number of fibers, the number of bundles, and the number of fibers in bundles in gastroc from the age- and gender-matched WT mice and untreated and TG-treated *HSA^{LR}* or DMSXL mice, MetaMorph (Molecular Devices) software was used as described previously (13, 17). The average cross section fiber area was examined in 100 to 300 fibers in the randomly selected fields from the matched areas of WT gastroc and untreated or treated *HSA^{LR}* and DMSXL gastroc. In the experiments using gastroc from hom DMSXL mice produced by the females treated with the vehicle, the measurements of the average fiber area and the number of fibers per view were corrected to the muscle weight, since the gastroc weight in these mice was reduced relative to that of hom DMSXL mice produced by the TG-treated females. The number of bundles, the number of fibers, and the number of central nuclei were determined in 6 to 12 views from the matched areas of gastroc at magnifications of $\times$10 or $\times$20.

Myoblast cell culture. Primary human myoblasts derived from three control patients without skeletal muscle pathology and from three patients with CDM1 (containing approximately 2,000 CTG repeats) were plated in 10-cm plates (approximately 5×10^7 frozen cells per plate) and maintained under the same conditions in the growth medium containing F10 medium (Gibco) supplemented with 15% fetal bovine serum (HyClone), 1% sodium bicarbonate (Gibco), 5% defined supplemental calf serum (HyClone), 1% L-glutamine (Gibco), and 1% penicillin-streptomycin (Gibco) at 60% density. To induce differentiation, myoblasts were grown to 80% density, and the growth medium was replaced with the fusion medium containing Dulbecco's modified Eagle's medium supplemented with horse serum and insulin for 2 to 5 days. Growth medium was changed every other day, and fusion medium was changed every day. The efficiency of differentiation was monitored by identification of multinucleated myotubes using bright-field microscopy and by IF assay using antibodies to skeletal muscle myosin chains 1 and 2 (Boster Biological Technology). In the IF assay, myotubes were grown on 1- or 2-chamber slides, and cells were fixed with 3.7% formaldehyde. After blocking in 1.5% bovine serum albumin (BSA) in phosphate-buffered saline (PBS) containing 1:100 goat serum, slides were incubated overnight with antibodies to myosin (1:150) and for 2 h with secondary antibodies labeled with fluorescein isothiocyanate (1:200). Nuclei were stained with 4′,6-diamidino-2-phenylindole (DAPI). The images were examined at $\times$40 magnification using a Nikon microscope.

Western blot analysis. Human myoblasts and myotubes were pelleted, and total protein extracts were purified with radioimmunoprecipitation assay (RIPA) buffer. Mouse muscle (gastroc or diaphragm) or the halves of whole brains were homogenized in RIPA buffer and total proteins were collected. Fifty micrograms of proteins was separated by SDS-gel electrophoresis, transferred onto membrane, and probed with antibodies according to the manufacturer's protocols. Antibodies to GSK3β, cyclin D3, PAX-7, and β-actin were from Santa Cruz Biotechnologies. Abs to RBM45 were from Sigma. Antibodies to desmin were from Abcam. In the co-IP experiments, CUGBP1 was precipitated from cytoplasmic extracts with 3B1 Abs, and the CUGBP1-IPs were examined by Western blotting with Abs to p51-eIF2α (Santa Cruz Biotechnologies).

Grip strength. The grip strength was examined using a grip strength meter from Columbus Instruments in the gender- and age-matched mouse groups as described previously (13, 17). Five measurements of the grip strength of the front paws were taken, and the average values are presented.

Open-field test. The open-field test was performed using the Open Field Superflex box with Fusion software, v5.3, from Omnitech Electronics (Columbus, OH). All measurements were performed in the same mouse room protected from noise and vibration. Mice were gently handled to reduce stress. Naïve

mice were placed in the center of the cage, and their movements were monitored for 5 min. The cage was washed with 70% ethanol after each test. Various parameters were determined, including total distance, total *x* axis distance, total *y* axis distance, vertical and horizontal movement time, vertical and horizontal activity counts, rest time, total movement time, total activity count, margin distance legacy, and central distance.

Splicing assay. Total RNA was extracted from tibialis anterior (TA) or gastroc of the matched WT and *HSA^{LR}* mice untreated and treated with TG or from human myotubes using TRIzol. The integrity of RNA was examined by gel electrophoresis. Reverse transcription was performed using 1 μg of total RNA and SuperScript III. The semiquantitative conditions of PCR were established using series of dilutions of 1 μl of reverse transcription mix with the internal standard primers for β-actin or glyceraldehyde-3-phosphate dehydrogenase. Human β-actin was used as a control for *BIN1* expression. The sequences of the human β-actin primers are 5′-TGACGGGGTCACCCACACTGTGCCCATCTA-3′ (forward) and 5′-CTAGAAGCATTTGC GGTGGACGATGGA-3′ (reverse). *BIN1* expression was examined with the *BIN1*-specific primers for the isoform lacking exon 11 under semiquantitative conditions established for β-actin. The sequence of the *BIN1* forward primer is 5′-AGAACCTCAATGATGTGCTGG-3′ and of the reverse primer is 5′-TCGTGGTTGA CTCTGATCTCGG-3′.

RT-PCR with these primers produced two *BIN1*-specific products with the inclusion and exclusion of exon 11. The RT-PCR products were separated on 4.5% agarose gel, and the intensities of the bands were quantified by the scanning densitometry using GAPDH or β-actin as a control. The amounts of the *BIN1* isoform lacking exon 11 were determined as a percentage of the total *BIN1* mRNA. The amounts of total *BIN1* mRNA were set at 100%.

Splicing assay assessing *Serca1* expression in TA and *Cypher* in gastroc of *HSA^{LR}* mice was controlled with *Gapdh*. The sequence of the forward primer for *Gapdh* is 5′-AACTTTGGCATTGTGGAAGGGCTC-3′. The sequence of the reverse primer is 5′-TGGAAGAGTGGGAGTTGCTGTTGA-3′. The splicing of *Serca1* was examined using primers for *Serca1* lacking exon 22, 5′-GCTCATGGTCCTCAAGATCTC-3′ (forward) and 5′-CACAGCTCTGCCTGAAGATG-3′ (reverse), under semiquantitative conditions established for *Gapdh*. The amounts of the *Serca1* mRNA isoform lacking exon 22 were determined as a percentage of the total *Serca1* mRNA. The amounts of total *Serca1* mRNA were set at 100%. The splicing assay examining the *Cypher* expression pattern was performed with the following primers as described previously (34): the sequence of the forward primer is 5′-GGAAGATGAGGCTGATGAGTGG-3′, and the sequence of the reverse primer is 5′-TGCTGACAGTGGTAGTGCTCTTTC-3′. The amounts of the WT specific *Cypher* isoform were determined as described above for *Serca1*.

Quantification of the mutant *DMPK* mRNA using Bpm1 polymorphism. Primary myoblasts from a pediatric patient with CDM1, containing approximately 2,000 CTG repeats, and a patient with the adult form of DM1, containing approximately 500 CTG repeats, were grown in the myoblast medium. Myoblasts were treated with 1.6 μg/ml TG two times a day apart. Total RNA was collected and subjected to the qRT-PCR with primers specific for the fragment of the exon 15 of *DMPK*, which contains a polymorphic site for Bpm1 enzyme. The sequence of the forward primer is 5′-CTGTCGGACATTCGGGA AGGT-3′, and the sequence of the reverse primer is 5′-CATCCTGTGGGGACACCGAGG-3′. The same amounts of the DMPK PCR products were subjected to digestion with Bpm1 overnight at 37°C, and the digest was analyzed by 12% polyacrylamide gel electrophoresis. The total amount of *DMPK* mRNA was set at 100%, and the percentages of the normal and mutant *DMPK* products were determined. Human GAPDH was used as a control. The sequences of GAPDH primers are the following: forward, 5′-CAATG ACCCCTTCATTGACC-3′; reverse, 5′-TTGATTTTGGAGGGATCTCG-3′.

Northern blot assay. Total RNA was extracted from gastroc of *HSA^{LR}* mice. RNA quality was verified by agarose gel electrophoresis. RNA samples (10 to 20 μg) were separated on the agarose gel containing 6% formaldehyde. RNA was transferred onto membrane and hybridized with ^{32}P-CAG$_{10}$ probe. After washing, the membrane was exposed to X-ray film. The membranes were reprobed with GAPDH as a control. The mutant CUG RNA in *HSA^{LR}* mice migrated as three isoforms with different lengths of CUG repeats. To quantify the mutant RNA in the vehicle- and TG-treated *HSA^{LR}* mice, the signals of all CUG-containing isoforms were summarized and the average CUG RNA levels were determined based on three experiments. The percentage of the mutant CUG RNA in the TG-treated mice was calculated using the average CUG RNA signal in the vehicle-treated *HSA^{LR}* mice set at 100%.

FISH assay. Untreated and TG-treated CDM1 myoblasts were fixed with 3.7% formaldehyde in PBS. Slides were prehybridized in 40% formamide and 2× SSC (1× SSC is 0.15 M NaCl plus 0.015 M sodium citrate) for 10 min at 37°C and hybridized overnight in the solution containing 40% formamide, 4× SSC, 1 mg/ml tRNA, salmon sperm DNA (200 μg/ml), 0.2% BSA, 2 μmol vanadyl guanoside, and 0.5 μg/ml CAG$_{15}$ probe labeled with Alexa555. The fluorescent signals were analyzed using the Nikon microscope under the same brightness and exposure time. The number of cells with and without CUG aggregates were determined in 40 random fields at ×40 magnification. The total number of analyzed cells was set at 100%, and the percentage of cells with CUG aggregates was calculated. The experiment was repeated 2 times using cells from two patients with CDM1.

Mouse muscle sections were prehybridized at 37°C in the solution containing 40% formamide and 2× SSC for 2 h. Hybridization was performed at 37°C in the solution of 40% formamide, 10% dextran sulfate, 2× SSC, and 30 ng/ml CAG$_{15}$ probe labeled with Alexa555 overnight. Following hybridization, sections were washed three times in 2× SSC and stained with DAPI. Images were examined on the Nikon microscope under the same time exposure and brightness. All CUG foci were counted in 100 to 120 randomly selected fibers in the vehicle- and TG-treated mice with two repeats of the experiment. The number of CUG foci in the vehicle treated mice was set at 100%.

qRT-PCR. Expression of *Rbm45*, *Mbnl3*, *Smn1*, and *Fgf-2* was examined under semiquantitative conditions described previously, using GAPDH as a reference (13). The sequences of the primers are as follows. For *Rbm45*, the forward primer is 5′-CTTGGGCTACGTGCGCTATT-3′ and the reverse primer is 5′-TATCCGATTCCCAGGAGGGT-3′. For *Smn1*, the forward primer is 5′-CCGAGCAGGAAGATACGGTG-3′ and the reverse primer is 5′-GTATGTGAGCACTTTCCTTCTTTTT-3′. For *Mbnl3*, the forward primer is 5′-TCCTTGAACCATCTGCAGTCA-3′ and the reverse primer is 5′-GTGAATCAAAACAGGCCACCA-3′. For *Fgf-2*, the forward primer is 5′-GGCTGCTGGCTTCTAAGTGT-3′ and the reverse primer is 5′-TTCTGTCCAGGTCC CGTTTT-3′. The lengths of the PCR products were 240 bp (*Mbnl3*), 832 bp (*Smn1*), 466 bp (*Rbm45*), and 163 bp (*Fgf-2*). The sequences of the mouse Gapdh primers were as described above for the splicing assay. The PCR products were separated on the 1 to 2% agarose or 12% polyacrylamide gels. The intensities of DNA bands were determined by scanning densitometry after adjustment to the intensity of Gapdh products. The experiments were repeated 4 to 6 times for each analyzed gene, and the average values were presented.

Statistical analysis. The intensities of the protein and RNA signals detected in Western blot, Northern blot, and qRT-PCR assays were determined by scanning densitometry relative to values for β-actin (for Western blot assay) or GAPDH and β-actin (for Northern blot and qRT-PCR assays). In the Northern blot assay, an additional control, such as the intensities of 28S and 18S RNAs, was used. Data were presented as means based on 3 to 6 repeats. Statistical analysis was performed using two-tailed Student's *t* test. A *P* value of <0.05 was considered statistically significant. Examination of treated cells and mice was blinded to the treatment.

ACKNOWLEDGMENTS

L.T. was supported by grants AR064488 and AR073379 and the CCHMC internal development fund. N.T. was supported by grants CA159942 and DK102597 and the internal development fund from CCHMC. Partial research support was from AMO Pharma Ltd.

The funders had no role in study design, data collection and interpretation, or the decision to submit the work for publication. M.S. is an employee of AMO Pharma Ltd. A.M. developed TG, which is patented by AMO Pharma Ltd. A.M. was a paid consultant to AMO Pharma.

M.W., W.-C.W., and L.S. performed experiments and analyzed and discussed data. D.L. performed brain analysis of DMSXL mice and discussed data. A.M., G.G., and M.S. provided critical reagents. N.T. discussed the results and provided conceptual advice. L.T. generated ideas and supervised all studies. L.T., N.T., and A.M. wrote the paper.

REFERENCES

1. Harper PS. 2001. Myotonic dystrophy. WB Saunders, London, United Kingdom.
2. Fu YH, Pizzuti A, Fenwick RG, Jr, King J, Rajnarayan S, Dunne PW, Dubel J, Nasser GA, Ashizawa T, de Jong P, Wieringa B, Korneluk R, Perryman MB, Epstein HF, Caskey CT. 1992. An unstable triplet repeat in a gene related to myotonic muscular dystrophy. Science 255:1256–1258. https://doi.org/10.1126/science.1546326.
3. Timchenko L. 2013. Molecular mechanisms of muscle atrophy in myotonic dystrophies. Int J Biochem Cell Biol 45:2280–2287. https://doi.org/10.1016/j.biocel.2013.06.010.
4. Miller JW, Urbinati CR, Teng-Umnuay P, Stenberg MG, Byrne BJ, Thornton CA, Swanson MS. 2000. Recruitment of human muscleblind proteins to (CUG)n expansions associated with myotonic dystrophy. EMBO J 19:4439–4448. https://doi.org/10.1093/emboj/19.17.4439.
5. Mankodi A, Logigian E, Callahan L, McClain C, White R, Henderson D, Krym M, Thornton CA. 2000. Myotonic dystrophy in transgenic mice expressing an expanded CUG repeat. Science 289:1769–1772. https://doi.org/10.1126/science.289.5485.1769.
6. Kanadia RN, Johnstone KA, Mankodi A, Lungu C, Thornton CA, Esson D, Timmers AM, Hauswirth WW, Swanson MS. 2003. A muscleblind knockout model for myotonic dystrophy. Science 302:1978–1980. https://doi.org/10.1126/science.1088583.
7. Timchenko NA, Cai Z-J, Welm AL, Reddy S, Ashizawa T, Timchenko LT. 2001. RNA CUG repeats sequester CUGBP1 and alter protein levels and activity of CUGBP1. J Biol Chem 276:7820–7826. https://doi.org/10.1074/jbc.M005960200.
8. Kuyumcu-Martinez NM, Wang G-S, Cooper TA. 2007. Increased steady-state levels of CUGBP1 in myotonic dystrophy are due to PKC-mediated hyperphosphorylation. Mol Cell 28:68–78. https://doi.org/10.1016/j.molcel.2007.07.027.
9. Timchenko NA, Patel R, Iakova P, Cai ZJ, Quan L, Timchenko LT. 2004. Overexpression of CUG triplet repeat-binding protein, CUGBP1, in mice inhibits myogenesis. J Biol Chem 279:13129–13139. https://doi.org/10.1074/jbc.M312923200.
10. Ho TH, Bundman D, Armstrong DL, Cooper TA. 2005. Transgenic mice expressing CUG-BP1 Reproduce splicing mis-regulation observed in myotonic dystrophy. Hum Mol Genet 14:1539–1547. https://doi.org/10.1093/hmg/ddi162.
11. Koshelev M, Sarma S, Price RE, Wehrens XH, Cooper TA. 2010. Heart-specific overexpression of CUGBP1 reproduces functional and molecular abnormalities of myotonic dystrophy type 1. Hum Mol Genet 19:1066–1075. https://doi.org/10.1093/hmg/ddp570.
12. Ward AJ, Rimer M, Killian JM, Dowling JJ, Cooper TA. 2010. CUGBPl overexpression in mouse skeletal muscle reproduces features of myotonic dystrophy type 1. Hum Mol Genet 19:3614–3622. https://doi.org/10.1093/hmg/ddq277.
13. Wei C, Stock L, Valanejad L, Zalewski ZA, Karns R, Puymirat J, Nelson D, Witte D, Woodgett J, Timchenko NA, Timchenko LT. 2018. Correction of GSK3β at young age prevents muscle pathology in mice with myotonic dystrophy type 1. FASEB J 32:2073–2085. https://doi.org/10.1096/fj.201700700R.
14. Huichalaf C, Sakai K, Jin B, Jones K, Wang G-L, Schoser B, Schneider-Gold C, Sarkar P, Pereira-Smith OM, Timchenko N, Timchenko L. 2010. Expansion of CUG RNA repeats causes stress and inhibition of translation in myotonic dystrophy 1 (DM1) cells. FASEB J 24:3706–3719. https://doi.org/10.1096/fj.09-151159.
15. Timchenko NA, Wang G-L, Timchenko LT. 2005. RNA CUG-binding protein 1 increases translation of 20-kDa isoform of CCAAT/Enhancer-binding protein beta by interacting with the alpha and beta subunits of eukaryotic initiation translation factor 2. J Biol Chem 280:20549–20557. https://doi.org/10.1074/jbc.M409563200.

16. Salisbury E, Sakai K, Schoser B, Huichalaf C, Schneider-Gold C, Nguyen H, Wang G-L, Albrecht JH, Timchenko LT. 2008. Ectopic expression of cyclin D3 corrects differentiation of DM1 myoblasts through activation of RNA CUG-binding protein, CUGBP1. Exp Cell Res 314:2266–2278. https://doi.org/10.1016/j.yexcr.2008.04.018.
17. Jones K, Wei C, Iakova P, Bugiardini E, Schneider-Gold C, Meola G, Woodgett J, Killian J, Timchenko NA, Timchenko LT. 2012. GSK3β mediates muscle pathology in myotonic dystrophy. J Clin Investig 122:4461–4472. https://doi.org/10.1172/JCI64081.
18. Naderi S, Gutzkow KB, Lahne HU, Lefdal S, Ryves WJ, Harwood AJ, Blomhoff HK. 2004. cAMP induced degradation of cyclin D3 through association with GSK-3 beta. J Cell Sci 117:3769–3783. https://doi.org/10.1242/jcs.01210.
19. Jones K, Jin B, Iakova P, Huichalaf C, Sarkar P, Schneider-Gold C, Schoser B, Meola G, Shyu AB, Timchenko N, Timchenko L. 2011. RNA foci, CUGBP1, and ZNF9 are the primary targets of the mutant CUG and CCUG repeats expanded in myotonic dystrophies type 1 and type 2. Am J Pathol 179:2475–2489. https://doi.org/10.1016/j.ajpath.2011.07.013.
20. Sabouri LA, Mahadevan MS, Narang M, Lee DS, Surh LC, Korneluk RG. 1993. Effect of the myotonic dystrophy (DM) mutation on mRNA levels of the DM gene. Nat Genet 4:233–238. https://doi.org/10.1038/ng0793-233.
21. Fugier C, Klein AF, Hammer C, Vassilopoulos S, Ivarsson Y, Toussaint A, Tosch V, Vignaud A, Ferry A, Messaddeq N, Kokunai Y, Tsuburaya R, Grange P, Dembele D, Francois V, Precigout G, Boulade-Ladame C, Hummel M-C, Munain AL, Sergeant N, Laquerrière A, Thibault C, Deryckere F, Auboeuf D, Garcia L, Zimmermann P, Udd B, Schoser B, Takahashi MP, Nishino I, Bassez G, Laporte J, Furling D, Charlet-Berguerand N. 2011. Misregulated alternative splicing of BIN1 is associated with T tubule alterations and muscle weakness in myotonic dystrophy. Nat Med 17:720–725. https://doi.org/10.1038/nm.2374.
22. Tamada H, Sakashita E, Shimazaki K, Ueno E, Hamamoto T, Kagawa Y, Endo H. 2002. cDNA cloning and characterization of Drb1, a new member of RRM-type neural RNA-binding protein. Biochem Biophys Res Commun 297:96–104. https://doi.org/10.1016/s0006-291x(02)02132-0.
23. Ogawa R, Ma Y, Yamaguchi M, Ito T, Watanabe Y, Ohtani T, Murakami S, Uchida S, De Gaspari P, Uezumi A, Nakamura M, Miyagoe-Suzuki Y, Tsujikawa K, Hashimoto N, Braun T, Tanaka T, Takeda S, Yamamoto H, Fukada S. 2015. Doublecortin marks a new population of transiently amplifying muscle progenitor cells and is required for myofiber maturation during skeletal muscle regeneration. Development 142:51–61. https://doi.org/10.1242/dev.112557.
24. Bourgeois F, Messéant J, Kordeli E, Petit JM, Delers P, Bahi-Buisson N, Bernard V, Sigoillot SM, Gitiaux C, Stouffer M, Francis F, Legay C. 2015. A critical and previously unsuspected role for doublecortin at the neuromuscular junction in mouse and human. Neuromuscul Dis 25:461–473. https://doi.org/10.1016/j.nmd.2015.01.012.
25. Huguet A, Medja F, Nicole A, Vignaud A, Guiraud-Dogan C, Ferry A, Decostre V, Hogrel JY, Metzger F, Hoeflich A, Baraibar M, Gomes-Pereira M, Puymirat J, Bassez G, Furling D, Munnich A, Gourdon G. 2012. Molecular, physiological, and motor performance defects in DMSXL mice carrying >1,000 CTG repeats from the human DM1 locus. PLoS Genet 8:e1003043. https://doi.org/10.1371/journal.pgen.1003043.
26. Tisdale S, Pellizzoni L. 2015. Disease mechanisms and therapeutic approaches in spinal muscular atrophy. J Neurosci 35:8691–8700. https://doi.org/10.1523/JNEUROSCI.0417-15.2015.
27. Panaite PA, Kielar M, Kraftsik R, Gourdon G, Kuntzer T, Barakat-Walter I. 2011. Peripheral neuropathy is linked to a severe form of myotonic dystrophy in transgenic mice. J Neuropathol Exp Neurol 70:678–685. https://doi.org/10.1097/NEN.0b013e3182260939.
28. Poulos MG, Batra R, Li M, Yuan Y, Zhang C, Darnell RB, Swanson MS. 2013. Progressive impairment of muscle regeneration in muscleblind-like 3 isoform knockout mice. Hum Mol Genet 22:3547–3558. https://doi.org/10.1093/hmg/ddt209.
29. Choi J, Dixon DM, Dansithong W, Abdallah WF, Roos KP, Jordan MC, Trac B, Lee HS, Comai L, Reddy S. 2016. Muscleblind-like 3 deficit results in a spectrum of age-associated pathologies observed in myotonic dystrophy. Sci Rep 6:30999. https://doi.org/10.1038/srep30999.
30. Kanadia RN, Urbinati CR, Crusselle VJ, Luo D, Lee YJ, Harrison JK, Oh SP, Swanson MS. 2003. Developmental expression of mouse muscleblind genes Mbnl1, Mbnl2 and Mbnl3. Gene Expr Patterns 3:459–462. https://doi.org/10.1016/S1567-133X(03)00064-4.
31. Yoshimura S, Takagi Y, Harada J, Teramoto T, Thomas SS, Waeber C, Bakowska JC, Breakefield XO, Moskowitz MA. 2001. FGF-2 regulation of neurogenesis in adult hippocampus after brain injury. Proc Natl Acad Sci U S A 98:5874–5879. https://doi.org/10.1073/pnas.101034998.
32. Lewis K, Valanejad L, Cast A, Wright M, Wei C, Iakova P, Stock L, Karns R, Timchenko L, Timchenko N. 2017. RNA binding protein CUGBP1 inhibits liver cancer in a phosphorylation-dependent manner. Mol Cell Biol 37:e00128-17. https://doi.org/10.1128/MCB.00128-17.
33. Hernández-Hernández O, Guiraud-Dogan C, Sicot G, Huguet A, Luilier S, Steidl E, Saenger S, Marciniak E, Obriot H, Chevarin C, Nicole A, Revillod L, Charizanis K, Lee KY, Suzuki Y, Kimura T, Matsuura T, Cisneros B, Swanson MS, Trovero F, Buisson B, Bizot JC, Hamon M, Humez S, Bassez G, Metzger F, Buée L, Munnich A, Sergeant N, Gourdon G, Gomes-Pereira M. 2013. Myotonic dystrophy CTG expansion affects synaptic vesicle proteins, neurotransmission and mouse behaviour. Brain 136:957–970. https://doi.org/10.1093/brain/aws367.
34. Kanadia RN, Shin J, Yuan Y, Beattie SG, Wheeler TM, Thornton CA, Swanson MS. 2006. Reversal of RNA missplicing and myotonia after muscleblind overexpression in a mouse poly (CUG) model for myotonic dystrophy. Proc Natl Acad Sci U S A 103:11748–11753. https://doi.org/10.1073/pnas.0604970103.
35. Jones K, Wei C, Schoser B, Meola G, Timchenko N, Timchenko L. 2015. Reduction of toxic RNAs in myotonic dystrophies type 1 and type 2 by the RNA helicase p68/DDX5. Proc Natl Acad Sci U S A 112:8041–8045. https://doi.org/10.1073/pnas.1422273112.
36. Latvanlehto A, Fox MA, Sormunen R, Tu H, Oikarainen T, Koski A, Naumenko N, Shakirzyanova A, Kallio M, Ilves M, Giniatullin R, Sanes JR, Pihlajaniemi T. 2010. Muscle-derived collagen XIII regulates maturation of the skeletal neuromuscular junction. J Neurosci 30:12230–12241. https://doi.org/10.1523/JNEUROSCI.5518-09.2010.
37. Wong LJ, Ashizawa T. 1997. Instability of the (CTG)n repeat in congenital myotonic dystrophy. Am J Hum Genet 61:1445–1448. https://doi.org/10.1086/301654.
38. Barbé L, Lanni S, López-Castel A, Franck S, Spits C, Keymolen K, Seneca S, Tomé S, Miron I, Letourneau J, Liang M, Choufani S, Weksberg R, Wilson MD, Sedlacek Z, Gagnon C, Musova Z, Chitayat D, Shannon P, Mathieu J, Sermon K, Pearson CE. 2017. CpG methylation, a parent-of-origin effect for maternal-biased transmission of congenital myotonic dystrophy. Am J Hum Genet 100:488–505. https://doi.org/10.1016/j.ajhg.2017.01.033.